urban science

MDPI

Article

Spatio-Temporal Hotspot Dynamics of Vulnerable and Protected Road Users in Coastal Tunisia

Fedy Ouni

Maritime Logistics & Supply Chain Management Department, Sharjah Maritime Academy, Khorfakkan P.O. Box 180018, Sharjah, United Arab Emirates; fedy.ouni@sma.ac.ae

Abstract

Road traffic crashes (RTCs) pose major public health and economic challenges, particularly in developing regions where protected road users (PRUs) and vulnerable road users (VRUs) may experience different patterns of collision risk. This study examines the spatial and temporal distribution of PRU and VRU collisions using a multi-stage geospatial analytical framework. The analysis uses five years of georeferenced collision data (2018–2022), comprising 4090 PRU and 3600 VRU incidents recorded along 3720 km of coastal roadways. Spatial and spatio-temporal methods, including hotspot analysis, space-time cube Emerging hotspot analysis, temporal heatmaps, and bivariate co-mapping, were applied to identify collision concentrations and their evolution over time. The results identified 144 significant PRU hotspots and 91 significant VRU hotspots, with concentrations particularly evident in the northern governorates. Emerging hotspot analysis further identified areas showing intensifying spatial concentrations of PRU and VRU collisions over the study period. Temporal patterns indicated distinct but partially overlapping collision patterns: PRU collisions were more concentrated during weekday commuting periods, while VRU collisions showed stronger daytime concentrations, with both groups exhibiting notable nighttime and weekend collision patterns. The spatial and temporal overlap between PRU and VRU collision hotspots indicates that some locations and periods experience elevated collision concentrations across different road-user groups. However, these concentrations should not be interpreted as exposure-adjusted measures of collision risk. The findings provide road-safety authorities with evidence to support spatially and temporally targeted investigations and more differentiated safety strategies for PRUs and VRUs, particularly in resource-constrained settings.

Keywords: road traffic crashes; vulnerable road users; protected road users; emerging hotspot analysis; spatio-temporal analysis; Tunisia

Check for updates

Academic Editors: Jieling Jin, Qiang Luo and Fangrong Chang

Received: 30 August 2026
Revised: 14 October 2026
Accepted: 19 October 2026
Published: 11 November 2026

Copyright: © 2026 by the author. Licensee MDPI, Basel, Switzerland. This article is an open access article distributed under the terms and conditions of the Creative Commons Attribution (CC BY) license.

1. Introduction

Road traffic crashes (RTCs) are increasingly emerging as a significant public health concern particularly in developing regions, posing a growing threat to community well-being. Annually, an estimated 1.2 million people lose their lives and over 50 million injuries due to RTCs, with projections suggesting that by 2030, RTCs could become the fifth leading cause of death [1]. The economic consequences are substantial, estimated to cost nations around 3% of their Gross National Product (GNP) [2]. This alarming trend has prompted numerous countries to implement safety measures aimed at mitigating road hazards and enhancing road safety [3].

While high-income nations have made notable progress in reducing RTCs, many low-income countries, particularly in Africa, still face significant challenges. This disparity highlights the urgent need for effective, evidence-based road safety strategies, particularly in resource-constrained settings. Despite commitments to international safety initiatives, financial constraints impede the implementation of effective countermeasures [4]. RTCs pose significant risks to all road users, but significant disparities exist in mortality rates among different groups.

Road users are classified into protected road users (PRUs) and vulnerable road users (VRUs) [5]. PRUs encompass operators and occupants of vehicles powered by engines, including passenger cars, trucks, buses, and commercial vehicles. While these users benefit from vehicle safety systems and structural protection, they remain at risk in high-speed collisions and when involved in crashes with larger vehicles or fixed objects. VRUs are defined as non-motorized road users who are at higher risk of injury or death when involved in traffic collisions due to their lack of external protection. Understanding these disparities is crucial for developing targeted interventions aimed at improving road safety for all users. The complexity of modern traffic environments requires comprehensive safety approaches that consider all road user types and their dynamic interactions across space and time.

Geographic information systems (GISs) have become indispensable tools in this analytical evolution, providing technological foundations for complex spatial analysis and visualization while enabling integration of diverse data sources including GPS-based incident locations, high-resolution imagery, traffic sensors, and demographic information [6]. Ref. [7] highlighted the widespread use of geospatial techniques, including hotspot mapping, spatial autocorrelation, and network-based risk assessment, to identify high-risk locations and underlying contributing factors. The integration of spatial and temporal dimensions has proven essential for understanding RTC patterns, as research consistently demonstrates that spatial-only or temporal-only analyses fail to capture the full complexity of traffic safety phenomena [8].

Despite the extensive application of GIS-based spatio-temporal analytical techniques for identifying RTC hotspots, important gaps remain in the literature. First, while baseline spatio-temporal analyses have effectively demonstrated regional clustering in various global contexts like Harbin [6] and major Californian cities [9] and confirmed the relevance of this analysis in Tunisia [3,10] and other African metropolitan cities [11], the existing body of literature often lacks the predictive specificity required for targeted policy intervention in complex demographic scenarios. Second, VRUs and PRUs are often analyzed together or without sufficient differentiation, which may obscure their distinct spatial and temporal patterns [12–14]. Third, the application of emerging hotspot analysis (EHA) to distinguish emerging, intensifying, persistent, and diminishing collision hotspots for different road-user groups remains limited, particularly in the context of Tunisian coastal regions. Addressing these gaps can provide more differentiated evidence to support road-safety planning and identify locations and periods that warrant further investigation. Accordingly, this study addresses the following research questions:

RQ1: How are PRU and VRU collisions spatially distributed and clustered across Tunisia's coastal road network?

RQ2: How do the temporal patterns of PRU and VRU collisions vary across years, days, and periods of the day?

RQ3: How do PRU and VRU collision hotspots evolve over space and time, and to what extent do their hotspot patterns overlap?

This study makes three main contributions. First, it examines PRU and VRU collisions separately rather than treating road users as a single aggregated group, thereby identifying differences in their spatial distributions and temporal collision patterns. Second, to the

authors' knowledge, it is the first study to apply emerging hotspot analysis to PRU and VRU collision data, enabling the identification of new, intensifying, persistent, and diminishing hotspots rather than a single static snapshot of risk. Third, it proposes a precision-oriented, multi-stage safety-management framework combining heatmaps, optimized hotspot analysis, emerging hotspot analysis, and bivariate co-mapping designed to remain operable in resource-constrained settings such as Tunisia's coastal regions.

The remainder of this paper is organized as follows. Section 2 presents a literature review. Section 3 summarizes the study area and data. Section 4 gives an overview of the methodology employed in the study, whereas Section 5 presents the empirical results and their discussions. Finally, Section 6 concludes the paper.

2. Literature Review

The non-random spatial distribution of RTCs has led to extensive research into identifying "black spots" or "hotspots," which are specific locations or road segments characterized by a disproportionately high crash concentrations [15]. Detecting such high-risk locations is critical for road-safety authorities as it enables the design of targeted interventions aimed at mitigating the likelihood of future RTCs [16]. Comparative analysis of hotspot identification practices across different countries reveals significant methodological heterogeneity in defining and delineating hotspots. Some European, Asian and African countries often apply varying thresholds, spatial units, and temporal windows to classify accident-prone sites. For example, Belgium and Austria rely primarily on frequency-based criteria, identifying hotspots with at least three serious or corporal crashes within 100–250 m over a one- to three-year period [17]. In contrast, Germany and Hong Kong integrate severity-weighted metrics, accounting for both fatal and serious crashes, and apply extended temporal windows of up to three years [18,19]. Flanders and Portugal apply composite indices combining injury types and gravity scores [18], thereby capturing the multidimensional nature of crash severity. Nordic countries such as Norway and Denmark introduce probabilistic and statistical approaches, including the Poisson test and gravity index thresholds to mitigate random fluctuations in crash occurrence [18]. Non-European practices exhibit similar diversity: Turkey employs a rate–quality–control model integrating accident rate, frequency, and severity; Malaysia uses accident density and weighted injury scoring [15]. In Tunisia, a hotspot is defined as any 1 km road segment recording at least ten serious or fatal crashes over five years [10]. These cross-national disparities highlight the lack of a unified standard and underscore the need for harmonized data-driven frameworks that balance statistical rigor with contextual adaptability in road safety diagnostics. The integration of GIS with advanced spatial analysis techniques has revolutionized the understanding of crash patterns, enabling more precise identification of high-risk locations and temporal concentrations.

GIS-based RTCs analysis lies in spatial point pattern analysis, which treats RTCs as discrete events distributed across geographic space. Spatial analytical techniques applied to RTCs fall into two main categories: distance-based and density-based approaches [20]. Distance-based approaches typically conceptualize crash data as linear events along road networks [21], most commonly as link features and encompass methods such as nearest neighbor distance analysis, Getis-Ord Gi* statistics, Ripley's K-function, and local Moran's I [22]. Density-based approaches analyze the precise geographic coordinates of crash events, with Kernel Density Estimation (KDE) recognized as the most widely adopted method due to its capacity to generate intuitive spatial visualizations and capture both micro-level clustering and macro-scale distributional patterns of RTCs [23].

Recent empirical investigations have increasingly underscored the methodological value and comparative strengths of these spatial analytical techniques. For instance, [24] performed a cross-city comparative spatial assessment of RTC patterns in Addis Ababa

(Ethiopia) and Berlin (Germany). The results revealed a pronounced spatial autocorrelation in Addis Ababa, indicative of a strong tendency for severe crashes to cluster geographically, whereas Berlin displayed comparatively weaker yet gradually strengthening spatial dependence. Local Moran's I analysis consistently identified High-High (HH) clusters predominantly located along major trunk roads in the city outskirts across both cities. Similarly, ref. [25] conducted a spatial clustering analysis in severity rates across Nepal's 77 districts over three fiscal years from 2019 to 2022, and to associate accident severity with road surface type. Their findings showed that districts with higher proportions of paved roads exhibited lower severity, whereas those with more earthen roads exhibited higher fatality clusters, particularly in remote areas such as Humla and Jumla. In the United States, ref. [26] investigated the spatial distribution and determinants of road traffic crash hotspots across Ohio through a combined geospatial statistical approach integrating KDE and spatial autocorrelation. Their findings revealed persistent hotspots in major cities, particularly Toledo, Columbus, Cleveland, and Cincinnati, with the most dangerous road sections in Cleveland, Toledo, Columbus, and Dayton. Critical findings indicated that High-High clusters identified by local Moran's I represent the highest priority areas for safety interventions, while Getis-Ord Gi* provides superior capability for distinguishing between hot areas requiring immediate intervention and cold areas representing baseline safety conditions. Ref. [9] integrated the Getis-Ord Gi* method with KDE to analyze the relationship between population density and crash occurrences in four major Californian cities confirming that statistically significant hotspots corresponded to areas with intense population concentration. Ref. [27] examined spatial autocorrelation of RTCs in Shiraz, Iran, with a specific focus on how clustering patterns vary by severity level. Using global and local spatial statistics, the authors found statistically significant spatial dependence across all crash severities, with severe crashes displaying stronger clustering tendencies than minor ones. Local Moran's I results identified distinct collision hotspots primarily along major arterial roads and intersections with high traffic exposure. Ref. [28] employed an integrated cluster analysis framework combining remote sensing, GIS, and Getis-Ord Gi* spatial statistics to examine road traffic incidents in Thanh Hoa Province, Vietnam (2020–2023). This approach successfully identified 64 significant hotspots, including 32 high-risk incident locations, thus illustrating the practical utility of spatial autocorrelation techniques in resource-constrained settings.

Recent studies have also extended spatial analysis to new user groups and emerging mobility modes. Ref. [29] analyzed e-bike crash severity and hotspots using a Random Parameter Logit model and Spatio-Temporal Network KDE. The findings revealed that elderly e-bike riders, intersections, and mixed traffic environments significantly increased severity. Moreover, the identified hotspots were strongly related to temporal travel patterns and the lack of physical segregation between roadway segments and intersections. Ref. [30] developed an integrated data-driven framework to assess cyclist risk and discomfort in Berlin using the GIS-based multi-criteria decision analysis (MCDA) approach. The results indicated that central Berlin exhibited both high cycling traffic density and elevated discomfort levels, with significant spatial correlations between these variables and land use patterns, particularly in commercial, educational, and residential zones. Moreover, high-risk cycling directions were found to align with areas of intense motor vehicle activity and specific urban land-use contexts. In a related study examining cyclist safety in complex urban environments, ref. [31] analyzed how infrastructure characteristics, traffic interactions, and spatial anomalies relate to cyclist risk in Rome, Italy, further illustrating how GIS-based spatial analysis can reveal context-specific risk patterns for vulnerable road users. Parallel advances have combined spatial autocorrelation with machine learning to enhance predictive accuracy and interpretability. Ref. [32] assessed how different road network

patterns influence traffic crash prediction performance by integrating geographic features into an interpretable machine-learning framework. Using a combination of spatial road network metrics, crash data, and explainable AI techniques, the authors demonstrated that the road network structure significantly affects both the likelihood and spatial distribution of crashes. Their interpretable model revealed that highly connected networks were associated with lower crash risks, whereas irregular and fragmented networks exhibited greater crash risks. Similarly, ref. [33] applied a Geographically Weighted Support Vector Machine (GW-SVM) framework combined with spatial autocorrelation approach to analyze and predict RTCs in California, integrating geospatial features, road network characteristics, and environmental factors. Results indicated that intersections, high-traffic corridors, and areas with complex road geometries were significant predictors of crashes. In a related application of machine-learning-enabled data analysis, ref. [34] used machine-learning techniques to predict road car accidents, further illustrating the growing role of data-driven predictive approaches in road-safety research.

Beyond spatial insights, temporal analysis complements spatial analysis by investigating how crash patterns evolve over time, enabling the detection of cyclical, seasonal, and daily trends in RTC frequencies and severities. Empirical findings consistently highlight distinct temporal patterns, indicating that road accidents often display pronounced seasonal variations, with accident frequencies peaking during festive periods or specific months linked to high traffic volumes or adverse weather conditions [6,35]. For example, ref. [6] reported higher crash frequencies in summer in Harbin, China, with medium- to high-density crashes concentrated near shopping malls, schools, and hospitals, particularly in summer and winter. Ref. [22] reported that crash rates tend to increase during rush hours, particularly in the morning and evening, and that weekends and summer months often experience higher frequencies of collisions. Ref. [36] reported that the relationship between socio-demographic, built environment, traffic exposure, and roadway characteristics with pedestrian crashes remains largely consistent throughout the day for both weekdays and weekends. Also, certain roadway types, such as secondary highways and major arterials, show a heightened risk at specific times of day. A study in Hyderabad, Pakistan, found that the largest number of RTA cases occurred in December, followed by July and November, indicating peaks during both winter and summer [35]. Ref. [37], in a ten-year analysis of U.S. crash data, found that despite an overall decrease in fatalities, the temporal risk patterns remained stable: weekends consistently had the highest fatalities, and the hours between 3 PM and 7 PM were the most dangerous on any given day. The study also highlighted elevated fatality rates on holidays like Independence Day and New Year's Day, often with higher alcohol involvement. Ref. [38] conducted a detailed evaluation of holiday effects on road crash casualties in the United Kingdom over a 28-year period. Their analysis revealed that crashes on public holidays were 16% more likely to result in killed or seriously injured (KSI) casualties. Specific holidays, such as New Year's Day and the Queen's Golden Jubilee in 2002, were associated with significantly higher KSI risks.

RTC patterns are dynamic, evolving in response to changes in traffic volume, land use, infrastructure improvements, and policy interventions. Recognizing this, recent research has advanced toward spatio-temporal methods that analyze how hotspots emerge, persist, intensify, or diminish over time. Among these, the co-map method provides a visual analytical tool designed to reveal how RTC hotspots change across both space and time. A key feature of the Co-map framework is its ability to identify season-related or time-specific hotspots by determining locations where crashes happen frequently only during certain periods [39]. Space–time cube (STC) further advances this line of analysis by aggregating events into a 3D grid structure over defined temporal intervals, where the x and y dimensions represent geographic space and the z dimension represents time [9,40].

Building on the STC, emerging hotspot analysis (EHA) combines the Getis-Ord Gi* statistic with the Mann–Kendall trend test to classify hotspot dynamics (e.g., new, consecutive, intensifying, persistent, diminishing, or sporadic) [40]. This provides a much more nuanced understanding of risk dynamics, enabling proactive rather than reactive safety management. Ref. [41] applied a STC analysis tool to identify hotspots of articulated heavy-vehicle crashes in Western Australia between 2001 and 2013. The findings showed that the majority of hotspots occurred in the vicinity or within the Perth metropolitan area. Based on spatial-temporal trend analyses, results revealed emerging hotspots with an increased level of significance throughout the time. By using the STC combined with EHA, ref. [12] examined how the spatio-temporal characteristics of crashes involving the elderly drivers and elderly victims in Seoul are changing by the time period. They found that the hot spots were clustered in specific areas during the morning to afternoon period. Also, hot spots are weak during winter and summer, whereas they are strong in the hiking and climbing areas in Seoul during spring and fall. Ref. [42] applied GIS-based spatio-temporal analysis for RTCs in Qatar between 2015 and 2019. The findings showed that weekday crashes in the central-eastern zone flipped from persistent to intensifying, while weekend crashes remained sporadic. Ref. [40] applied an EHA for a 16-year series (2005–2020) of injury-severity-weighted crashes on Ghana's trunk roads. They found intensifying hotspot locations where crash severity was statistically increasing over time concentrated in rural areas and on key corridors between major cities like Accra and Kumasi. Ref. [9] employed space–time cube analysis to visualize the dynamics of accident occurrences in four Californian cities, revealing distinct annual and geographic patterns. For instance, the analysis showed persistent, dense clustering in Los Angeles across all years, while highlighting an emerging spike in crashes in San Jose in 2021. Recently, ref. [43] applied a STC on a major freeway corridor in the United States, covering a four-year period across 20 counties. The findings showed that persistent hotspots appeared more frequently in major freight hubs and urban areas while sporadic hotspots were clustered in rural corridors. Ref. [8] used the global Moran's I index to investigate spatio-temporal clustering of RTCs in the Bangkok Metropolitan Region over a 10-year period. By applying the analysis across multiple time scales (time of day, day of week, month), they confirmed that crash clusters were statistically significant and that their patterns varied markedly between daytime, nighttime, and festive seasons.

Although GIS-based hotspot detection and spatio-temporal analysis are established approaches in road-safety research, their combined application to distinguish the spatial and temporal patterns of PRU and VRU collisions remains insufficiently documented in the context examined here. Previous research by Ouni and Belloumi [3,10,44] provides an important foundation for geospatial road-safety analysis in Tunisia; however, the present study extends this line of research by examining PRU and VRU collision patterns separately and integrating spatial hotspot detection, emerging hotspot classification, temporal analysis, and bivariate co-mapping within a single analytical application. The contribution lies not in proposing new GIS algorithms, but in the comparative application of established methods to characterize the spatial distribution, temporal variation, and potential overlap of collision concentrations among different road-user groups across Tunisia's coastal regions.

3. The Study Area and Data Collection

The study focuses on Tunisia's coastal regions, encompassing the governorates of Nabeul, Sousse, Monastir, Mahdia, and Sfax. Census results reveal that these governorates collectively house nearly two-thirds of the country's population, making them among the most densely populated in Tunisia. As key hubs of cultural, social, and economic activity, they play a crucial role in national development. The region's geographic location, stretching from the north to the east, provides a strategic advantage, supporting a wide

range of economic activities. The coastal zone accounts for over 80% of Tunisia's economic output, more than 90% of its tourist accommodation capacity, and a sustains a significant share of its irrigated agriculture. Furthermore, the coastal zone serves as a primary gateway for international trade, featuring nine ports, an oil terminal, and six international airports. This concentration of infrastructure and economic activity drives higher mobility demands along the coast compared to inland regions, resulting in increased motorization rates among coastal populations. Traffic and congestion are often experienced in the coastal regions as a result of the influx and outflux flows of vehicles. This study uses geo-referenced collision records involving VRUs and PRUs that resulted in casualties along the coastal region in Tunisia over the recent 5 years from 2018 to 2022. Data were obtained from the National Observatory for Road Safety (NORS) and restricted to police-reported casualty collisions (fatal and injury-related crashes); Property-Damage-Only (PDO) collisions were excluded due to inconsistent reporting standards. Each record in the dataset represents a unique crash event rather than individual victims. Where a single crash involved multiple casualties, it was recorded as a single spatial incident. Fatal and non-fatal injury crashes were analyzed together as aggregated collision events to maintain statistical power across spatial units. Data quality control involved rigorous preprocessing: duplicate entries were identified and removed by screening for identical incident timestamps, road numbers, and linear markers. Records with missing or unresolvable spatial references were excluded. Detailed distribution of PRU and VRU collisions across Tunisian coastal regions for each year between 2018 and 2022 is presented in Appendix A. Consequently, 4090 PRU and 3600 VRU collision records within the survey period were used for this study. For spatial analysis purposes, PRU and VRU locations were georeferenced using the World Geodetic System 1984 (WGS84) coordinate framework and projected onto highway layout data. The spatial positioning process utilized route designations and stone-marker references, integrated with highway geographic information system (GIS) layers through ArcGIS 10.6 linear referencing functionality. The collected highway data includes freeways, national highways (NH), regional highways (RH) and local highways (LH) but excludes municipal highways and railways. Unlike previous studies that relied on hypothetical corridors or selectively examined limited highway segments, the present study employs a comprehensive and fully geocoded road network dataset comprising approximately 3720 km of classified roads, including 130 km of freeways, 834 km of NH, 1800 km RH, and 956 km of LH. Much of the traffic flow within the study area utilizes the national and regional highways. NH are major roads that connect large cities and economic centers. They are designed to handle higher traffic volumes and facilitate rapid travel between regions. RHs, on the other hand, are secondary roads that connect less densely populated areas or rural regions to NHs and urban centers. They are often used for local and regional transport, thereby contributing to better regional integration. In the NORS database, collisions are originally recorded under a more granular set of road-user categories, including pedestrians, cyclists, motorcyclists/moped riders, passenger-car occupants, bus/minibus occupants, truck occupants, and other motorized-vehicle occupants. For the purposes of this study, pedestrians, cyclists, and motorcyclists/moped riders were merged into the VRU category, consistent with the internationally recognized definition of vulnerable road users as those lacking an external protective structure [5]. Passenger-car, bus, truck, and other motorized-vehicle occupants were merged into the PRU category. Regarding geocoding quality, PRU and VRU records were matched to the road network using route designation and stone-marker (kilometer-post) references rather than raw GPS coordinates. This route-and-marker referencing approach is not subject to GPS positional error, but its accuracy is bounded by the precision of the marker value recorded in the police report. As with any analysis built on police-reported crash data, the dataset is also subject to underreporting, particularly for

minor collisions that do not involve severe injury and may not be formally recorded. In addition, the dataset used in this study did not provide sufficiently complete and consistent information for several potentially relevant exposure and contextual variables, such as traffic volume, road-user exposure, weather conditions, lighting conditions, road-surface condition, vehicle speed, and individual characteristics such as age. These variables were therefore not incorporated into the hotspot analyses. Consequently, the results should be interpreted as describing the spatial and temporal concentration of reported collisions rather than exposure-adjusted crash risk or causal effects of specific road or behavioral factors.

Figure 1 illustrates the study area with the locations of PRU and VRU collisions from 2018 to 2022. To examine the spatial distributional tendencies and directional patterns of PRU and VRU collision occurrences, a Standard Deviational Ellipse (SDE) was generated using the Directional Distribution tool in ArcGIS 10.6, summarizing dispersion and orientation relative to the mean center. The resulting spatial pattern, presented in Figure 1, indicates that PRU and VRU collision concentration and the distribution of injuries and fatalities follow a predominantly north-west to south-west orientation along the coastal axis.

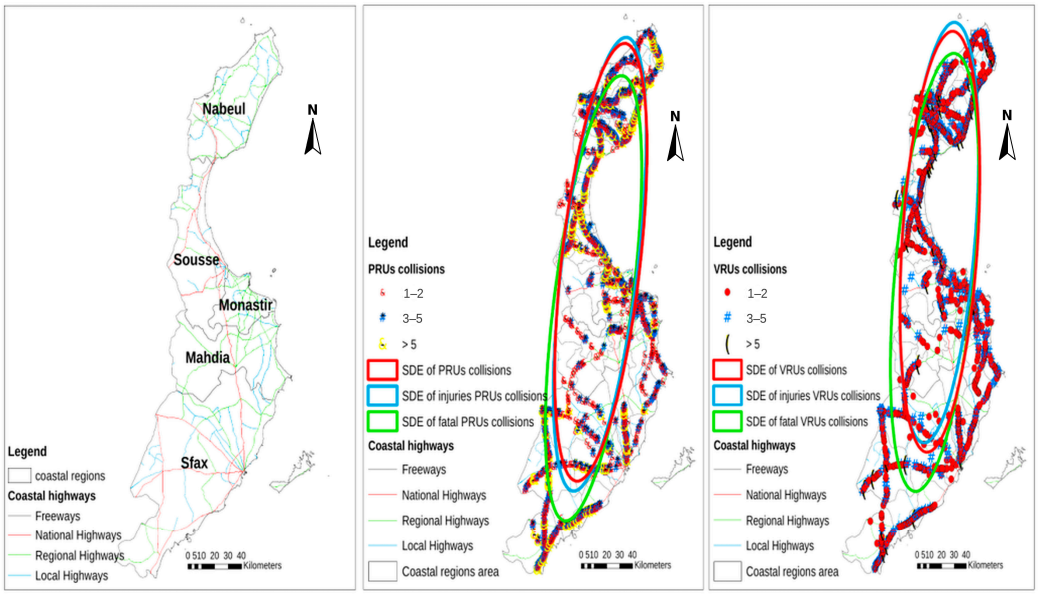

Figure 1. Study area and spatial distribution of PRUs and VRUs collisions from 2018 to 2022.

4. Methodology

The overall methodological framework is illustrated in Figure 2. Following data preprocessing, complementary GIS-based techniques are applied to examine the spatial, temporal, and spatio-temporal patterns of collisions involving PRUs and VRUs. Each technique addresses a specific analytical objective, from identifying spatial hotspots and visualizing collision concentrations to examining temporal variations, hotspot evolution, and spatial overlap between the two road-user groups. The results are interpreted jointly to provide a comprehensive understanding of collision patterns across Tunisia's coastal road network. The following subsections describe each analytical method in detail.

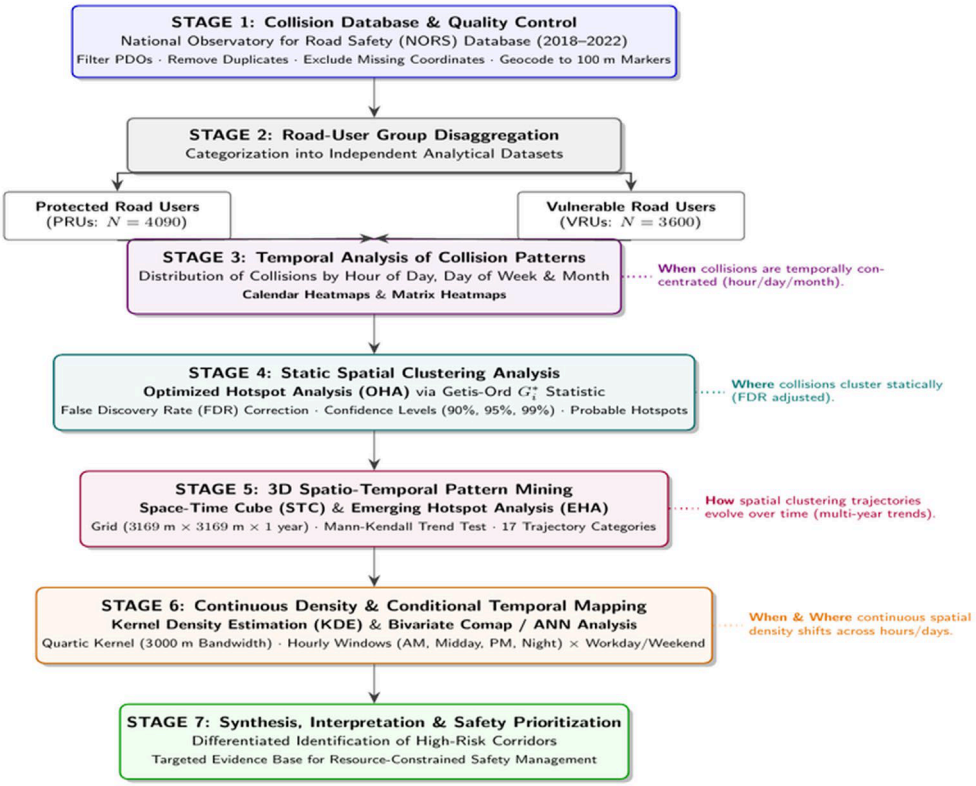

Figure 2. Methodological flowchart.

4.1. Heatmap Visualization Analysis

To effectively illustrate the temporal patterns of PRU and VRU collisions, it is essential to utilize visualization techniques that integrate multiple time dimensions. Representing accident occurrences through formats such as calendar charts, time matrices, and polar coordinate graphs provides a clearer and more comprehensive understanding of when accidents are most frequent [45]. Among these, calendar-based visualizations and matrix heatmaps are particularly useful, as they organize accident data into structured time intervals, facilitating the identification of trends across hours, days, or months. Calendar heatmaps are particularly useful for visualizing temporal patterns, such as accident rates over days or months, and have been applied to road traffic accident analysis to uncover hidden time-based trends [46]. These visualization methods are crucial for road safety analysis, as they support data-driven decision-making, enabling targeted interventions and policy adjustments aimed at reducing RTC occurrences.

4.2. Optimized Hotspot Analysis

The optimized hotspot analysis (OHA) represents an advanced geostatistical approach developed to detect, measure, and validate local spatial autocorrelation in incident data while simultaneously addressing issues arising from multiple hypothesis testing and spatial dependency. To mitigate the inflated false-positive rate that arises from conducting repeated local significance tests across numerous spatial units, the OHA incorporates the False Discovery Rate (FDR) correction, which adjusts the statistical significance thresholds to account for multiple spatial comparisons, and thereby enhances the reliability and robustness of hotspot detection [47]. The OHA follows a multi-stage analytical process that begins with intelligent spatial aggregation of RTC data through hexagonal tessellations or fishnet grids to reduce spatial bias and support local neighborhood–based inference. PRU and VRU collision events are first enumerated within these predefined spatial units, after

which local spatial autocorrelation statistics are applied to assess collision concentration and statistical significance of clustering. The analytical framework automatically determines optimal spatial scales of analysis through iterative optimization procedures that balance spatial resolution requirements against statistical power considerations and minimizing false positives. The output surface therefore visualizes localized hotspot and coldspot patterns, allowing for fine-grained spatial differentiation of collision risk. The OHA tool uses the Getis-Ord Gi* statistics. Under the null hypothesis spatial randomness H_0, it is assumed that no spatial clustering exists, and the observed spatial distribution of collision counts within the study area is random. For a given spatial feature i, the Gi* statistics within a scale distance d is defined as:

$$G_i^* = \frac{\sum_{j=1}^{n} w_{ij}x_j - \overline{X}\sum_{j=1}^{n} w_{ij}}{S\sqrt{\frac{n\sum_{j=1}^{n} w_{ij}^2 - \left(\sum_{j=1}^{n} w_{ij}\right)^2}{n-1}}}, \ \forall\, i \neq j \quad (1)$$

$$\overline{X} = \frac{\sum_{j=1}^{n} x_j}{n} \quad (2)$$

$$S = \sqrt{\frac{\sum_{j=1}^{n} x_j^2}{n} - \left(\overline{X}\right)^2} \quad (3)$$

where x_j represents the attribute value associated with spatial feature j, w_{ij} denotes the spatial weight coefficient between features i and j, X corresponds to the mean attribute value across all spatial units, S represents the standard deviation of attribute values and n indicates the total number of spatial units under analysis. The expected value E(Gi*) under H_0 is given by:

$$E(G_i^*) = -\frac{\sum_{j=1}^{n} w_{ij}}{n-1} \quad (4)$$

The Getis-Ord Gi* analysis produces a map in which each cell is attributed a z-score and an associated p-value, enabling statistical interpretation of spatial clustering patterns. High positive z-scores coupled with low p-values identify statistically significant clusters of high collision intensities (hotspots), whereas high negative z-scores with low p-values indicate significant clusters of low collision intensities (coldspots). Z-scores close to zero denote the absence of spatial clustering [48]. Conventionally, standard normal z-scores of ±1.65, ±1.96, and ±2.58 correspond to two-tailed statistical confidence levels of 90% ($p < 0.10$), 95% ($p < 0.05$), and 99% ($p < 0.01$), respectively. In the ArcGIS optimized hotspot analysis implementation, p-values and z-scores are automatically adjusted using the False Discovery Rate (FDR) correction to account for spatial autocorrelation and multiple testing constraints. Consequently, features classified as statistically significant hotspots meet or exceed the adjusted critical threshold of $z \geq 1.645$ (90% confidence level) [3]. In addition, following [3,49], locations with positive z-scores between 1.002 and 1.645 were classified as probable hotspots. This supplementary category was retained to identify potential concentrations of collisions that did not reach the conventional 90% confidence threshold. Accordingly, probable hotspots were treated as an exploratory classification rather than statistically significant clusters.

4.3. Emerging Hotspots Analysis

The emerging hot spot analysis approach enhances conventional hot spot analysis methods by including time. Investigating collision data over space and time can reveal significant trends that improve the knowledge of changing landscapes. Previous case studies spanning the Gulf regions [42], Sub-Saharan Africa [40], Oceania [50] and North America [43] confirm that the space–time cube method reliably pinpoints where and when

crash risk is escalating, delivering actionable intelligence that conventional 2-D hotspot tools miss. In this study, the space–time pattern mining tool available in ArcGIS 10.6 was employed to identify and categorize the spatial-temporal trends of PRU and VRU collision patterns within a study region. Before running statistical analysis, a space–time cube is generated by summarizing point data into space–time bins structured into a netCDF format (Network Common Data Form) data cube. To create a space–time cube, authors at least define a time-step interval and a distance interval that will define the bin dimensions for aggregating collision data. The time-step interval option defines the time period for each bin. The distance interval specifies the spatial dimensions of the bins that stretch through the study area as a fishnet grid location. The generated structure is a three-dimensional space–time cube composed of bins that each characterize a fixed position in space (x, y) and in time (t) [41]. In this study, the value of space (x, y) was 3169 m by 3169 m square, which was calculated by dividing the longest side of the study area (316,900 m) by 100. It is essential to create a field of type 'Date' in the attribute table of PRU and VRU collision data as this field will aggregate points directly into bins by time. Each of the time-step intervals is 1 year in duration to assess changes in PRU and VRU collisions from year-to-year, so the entire time period covered by the space–time cube is 5 years from 1 January 2018, to 31 December 2022, a period long enough to reduce random fluctuation. Hence, all times included in this analysis fall between those dates. Bins covering the same (x, y) area share the same location ID, and bins covering the same duration share the same time-step ID [41]. The choice of a 3169 m × 3169 m spatial bin and a one-year temporal step was guided by ArcGIS's default space–time cube sizing rule, which divides the longest side of the study extent by 100 to balance the number of bins against the number of points available per bin, combined with a one-year step reflecting the annual reporting cycle of the NORS database and the five-year span of the dataset.

The points are counted within each bin and the trend for bin values is calculated over time at each location using the Mann–Kendall statistic [41]. The Mann–Kendall trend analysis is a non-parametric statistical test range from −1 to +1 used to test whether a statistically significant temporal trend exists through each bin's five-year time series of z-scores and *p*-value resulting from the Getis-Ord Gi* statistic (Equations (1)–(3)). The benefits of the Mann–Kendall trend test over Spearman's rho test is that it is less affected by restricted numbers of extreme outliers, and it can even work with missing data.. The output of the emerging hotspot tool categorizes the results into 17 categories indicating the temporal trends of hot and cold spots over time. A category was assigned to each bin to further describe the occurring trend. Overall trend values can reveal many changes in PRU and VRU patterns within the 5-year period of this study. Once the space–time hot spot analysis was executed, each location was given a z-score and *p*-value, and a hot spot classification was assigned to it. Lastly, two-dimensional visualization was utilized to provide users with a more realistic picture of PRU and VRU hot spot characteristics and dynamics over a time-revealing trend direction rather than a static heatmap.

4.4. Co-Map Method

The co-map method is an extension of Cleveland's co-plot method functioning as an exploratory cartographic-statistical approach for examining the relationships between a pair of variables and their variation over time [20]. Introduced by [51] for crime mapping, the co-map approach has increasingly been adopted in several spatio-temporal accidents analysis studies [6,20,27,52–54]. The co-map method works by subdividing aggregated crash data according to specific time periods and then analyzing the density of each subset using KDE [20]. The results are presented in various maps or plots arranged successively to show how the spatial distribution of traffic accidents changes over time [20]. KDE is

a widely recognized non-parametric spatial analysis technique used to describe the first-order properties of point-pattern data [55]. The underlying premise of this method is that the spatial point pattern exhibits a continuous probability density across the study area, rather than only at the discrete locations where crashes are observed [10]. KDE produces a continuous, smooth surface depicting the spatial concentration of events by assigning higher weights to nearby points more than far ones based on a selected kernel function. The general formulation of KDE is expressed as:

$$f(x, y) = \frac{1}{nh^2} \sum_{i=1}^{n} K\left(\frac{d_i}{h}\right) \quad (5)$$

where $f(x, y)$ denotes the estimated density at location (x, y), n is the total number of crash events, $h > 0$ is the smoothing parameter or bandwidth, $K(.)$ denotes the kernel function, and d_i is the Euclidian distance between the location (x, y) and the ith event location. Various kernel functions have been adopted in spatial analysis such as Gaussian, Quartic, Negative Exponential, Triangular, and Epanechnikov, each offering distinctive smoothing properties [44]. In this study, the Quartic kernel function provided in ArcGIS 10.6 was employed. Its mathematical form is given by:

$$k\left(\frac{d_i}{h}\right) = K\left(1 - \frac{d_i^2}{h^2}\right) \quad \text{when} \quad 0 < d_i \leq h \quad (6)$$

$$k\left(\frac{d_i}{h}\right) = 0 \quad \text{when} \quad d_i > h \quad (7)$$

In Equation (6), K represents the kernel function, h denotes the bandwidth and d_i is the distance between the location (x, y) and the location of the ith crash. In Equation (7), the kernel value becomes zero for events located beyond the bandwidth threshold. The selection of bandwidth length is a critical parameter in KDE for accurately identifying accident hotspots, as it significantly influences the smoothness and detail of the density estimate [56]. A smaller bandwidth yields a highly localized density surface, highlighting very specific areas of high RTC concentration. While this can reveal fine-grained hotspots, it also increases sensitivity to random spatial fluctuations, which may result in the identification of statistically insignificant or noise-driven clusters. In contrast, applying a larger bandwidth produces a more smoothed density surface that captures broader spatial trends in RTC distribution. While such smoothing enhances the ability to discern overarching high collision concentration zones, it might obscure smaller, yet significant, localized hotspots within those broader regions [57]. Following exploratory calibration, a bandwidth of 3000 m and a raster cell size of 1000 m were selected for the density mapping in this study to ensure an optimal balance between spatial precision and pattern interpretability. When coupled with tests like Moran's I, Average Nearest Neighbor analysis or Gi*, KDE results become more robust by filtering out clusters that lack statistical significance, improving hotspot reliability [54].

5. Results

5.1. Temporal Analysis

Figure 3 displays calendar heatmaps depicting the daily fluctuations in PRU and VRU collisions and fatalities over multiple years.

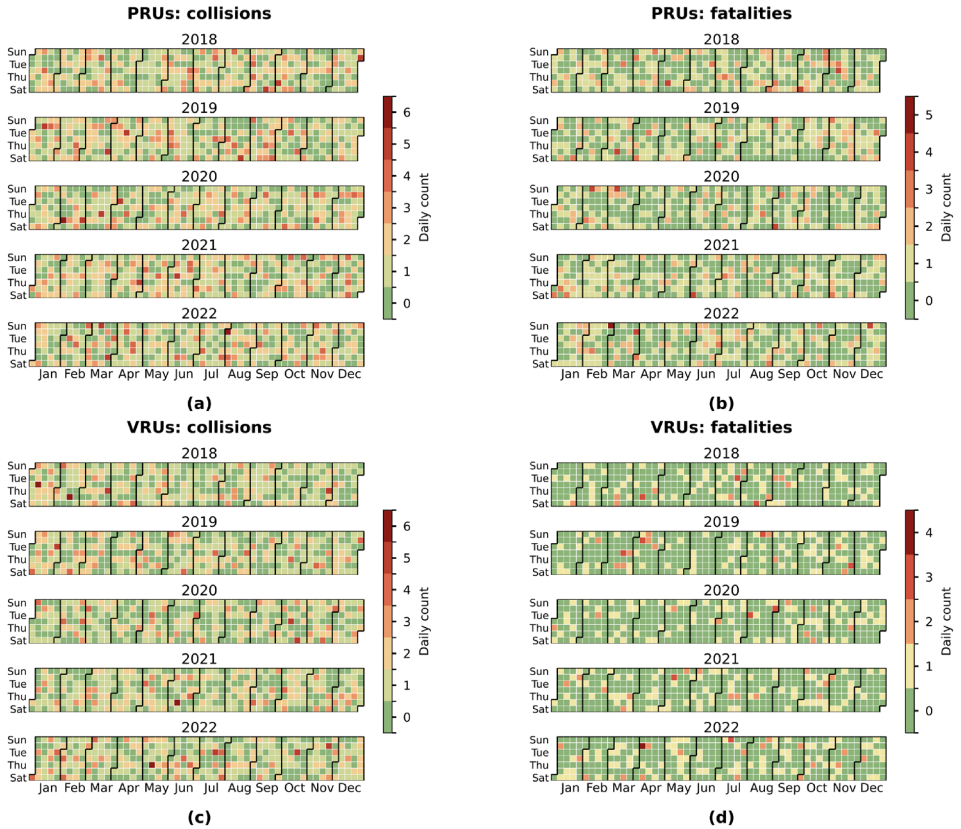

Figure 3. Calendar heatmaps of collisions between 2018 and 2022. (**a**) Calendar heatmap of PRU collisions. (**b**) Calendar heatmap of PRU fatalities. (**c**) Calendar heatmap of VRU collisions. (**d**) Calendar heatmap of VRU fatalities.

As shown in Figure 3, PRU collisions generally exhibit sporadic peaks, particularly toward the end of each year, which may be linked to increased travel activity, holiday-related congestion, and adverse weather conditions. In contrast, VRU collisions are more evenly distributed throughout the year, suggesting that VRUs are consistently exposed to road risks regardless of seasonal variations [10]. PRU collisions occur more frequently but still remain lower in intensity than VRU collisions, indicating that while PRUs are involved in crashes, they have a lower fatality rate. Across all years, 2020 shows a decline in incidents, likely due to COVID-19-related mobility restrictions. Weekly patterns indicate that collisions and fatalities are spread throughout the week, though certain days show higher spikes (dark red cells), possibly due to commuting patterns.

Figure 4 presents six matrix heatmaps illustrating the temporal distribution of PRU and VRU collisions. Each heatmap is structured with hours of the day on one axis and days of the week on the other, enabling the temporal distribution of collision frequency, injuries, and fatalities to be examined.

The matrix heatmaps reveal distinct temporal patterns of road traffic outcomes for PRUs and VRUs. PRU collisions and injuries are concentrated during weekday morning and evening peak hours, whereas PRU fatalities are more dispersed across the weekly and hourly periods. For VRUs, collisions and injuries are predominantly distributed during daytime hours, particularly during the mid-morning and late-afternoon periods, while VRU fatalities show greater concentration during late-night hours and weekends. Overall, the temporal analysis indicates distinct distributions of collision occurrences across hours and days for PRUs and VRUs, with differences between collision, injury, and fatality patterns.

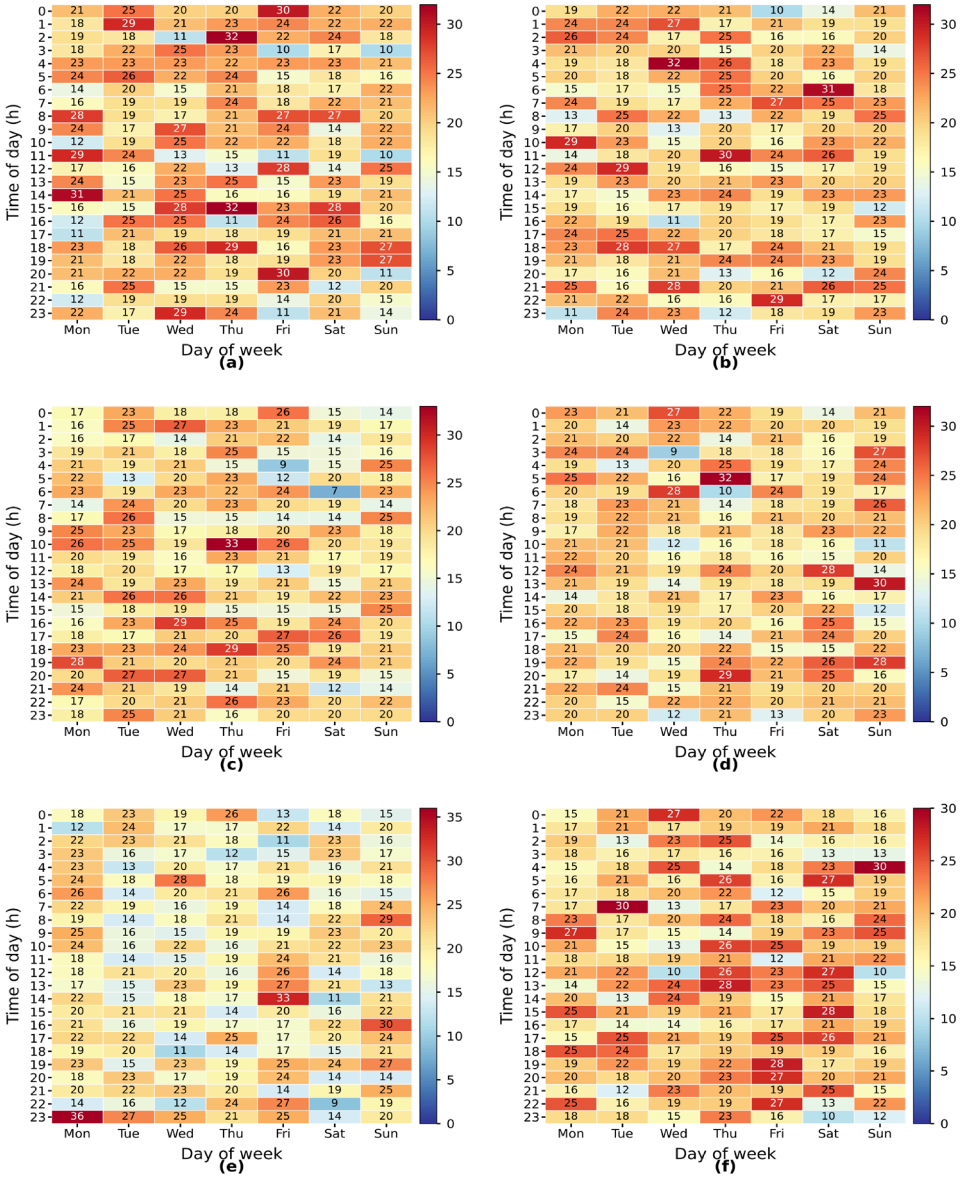

Figure 4. Matrix heatmap of collisions by hours and day of week. (**a**) PRU collisions. (**b**) PRU injuries. (**c**) PRU fatalities. (**d**) VRU collisions. (**e**) VRU injuries. (**f**) VRU fatalities.

5.2. Optimized PRU and VRU Hotspot Analysis

The comprehensive geospatial analysis depicted in Figure 5 revealed 144 statistically significant PRU hotspots and 91 VRU hotspots across the 90%, 95%, and 99% confidence levels, demonstrating substantial spatial heterogeneity in collision distribution patterns.

The spatial distribution analysis reveals a pronounced concentration of both PRU and VRU hotspots in the northern portions of the study area, particularly within the Nabeul and Sousse governorates, while Monastir and Mahdia exhibited no statistically significant hotspot occurrences. Since Gi* z-score can be measured for each fishnet grid, it can be used as a quantitative dangerousness index, enabling objective risk assessment and prioritization across spatial units. Grid cells exhibiting the highest z-score values represent locations with maximum concentration, while those with the smallest z-scores indicate areas of relatively low collision risk. This approach actually zooms into the locations requiring immediate investigative attention and intervention prioritization. The analysis identified 62 grid cells for PRUs and 85 grid cells for VRUs with z-scores > 2.58 and p-values < 0.01. These locations

represent the highest collision concentration zones with 99% statistical confidence level and were ranked in ascending order according to a dangerousness index.

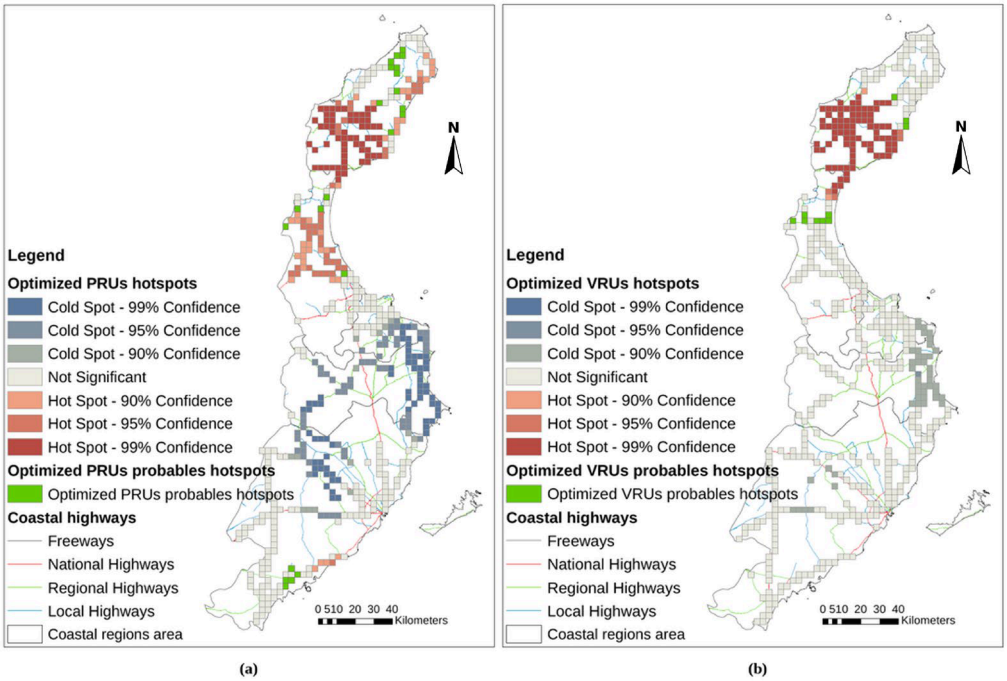

Figure 5. (**a**) Optimized PRU and (**b**) VRU hotspots and probable hotspots.

Figure 5 provides a fine-scale geospatial representation of the most critical PRU and VRU hotspot locations. Detailed examination of the highest-risk hotspots as visualized in Figure 6 reveals distinct spatial clustering patterns concentrated around specific geographical features.

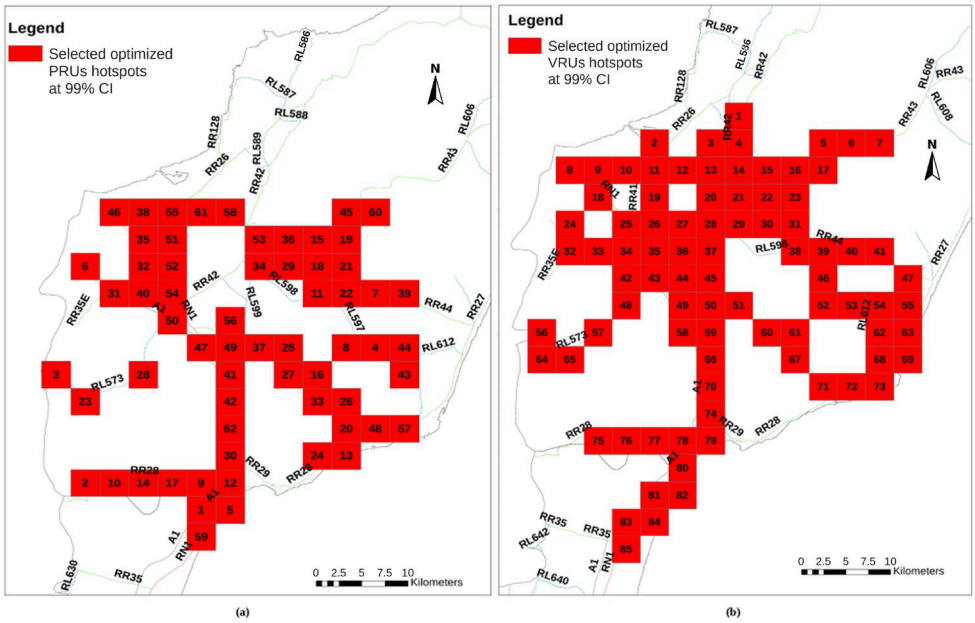

Figure 6. Fine-scale geospatial view of most critical (**a**) PRU and (**b**) VRU hotspots.

The critical hotspot locations were concentrated mainly within the Nabeul governorate, particularly along major transportation corridors including national highway 1 (NH1)

and regional highways 28, 29, 42, 43, and 44. Hotspot concentrations were also identified around major road junctions, including the intersections of NH1 with RH28 and NH1 with RH42. The spatial analysis further identified probable or potential hotspots based on the study-specific z-score range of 1.002 to 1.645. PRU probable hotspots showed a relatively widespread regional distribution, with concentrations in the northern and southwestern portions of the study area. VRU probable hotspots exhibited a more concentrated spatial distribution, primarily in the Nabeul region and in the vicinity of the Sousse governorate. Overall, the optimized hotspot analysis identified distinct spatial concentrations of PRU and VRU collisions across the study area, with the most pronounced concentrations occurring in the northern coastal region. The spatial distributions of the two user groups showed both common hotspot locations and differences in the extent and concentration of their respective hotspot patterns.

5.3. Emerging PRU and VRU Hotspot Analysis

The emerging hotspot analysis (EHA) was applied to the PRU and VRU collision data to characterize the spatial and temporal patterns of collision hotspots over the five-year study period.

For emerging PRU hotspots, the space–time cube has aggregated 4090 points into 3500 locations over 5-time-step intervals. Of the 3500 total locations, 487 (13.91%) contain at least one point for at least the one-time-step interval. These 487 locations comprise 6331 space–time bins of which 3050 (48.17%) have point counts greater than zero. According to the two-tailed Mann–Kendall trend test, PRU point counts show a statistically significant decreasing trend over time at the conventional $\alpha = 0.05$ level (trend statistic = −2.109, trend p-value = 0.03).

For emerging VRU hotspots, the space–time cube has aggregated 3600 points into 3600 fishnet grid locations over 5-time-step intervals. Of the 3600 total locations, 475 (13.19%) contain at least one point for at least one-time-step interval. These 475 locations comprise 6175 space–time bins of which 1857 (30.07%) have point counts greater than zero. The Mann–Kendall test for VRU point counts yields a negative trend statistic (−1.647, $p = 0.09$) that does not reach conventional statistical significance at $\alpha = 0.05$. The result therefore does not provide sufficient statistical evidence to conclude that a monotonic temporal trend exists.

The emerging hotspot analysis identified statistically significant hot/cold trends in 81.31% of the space–time bins analyzed for PRUs and 49.68% for VRUs. The resulting two-dimensional emerging hotspot maps for PRUs and VRUs are presented in Figure 7, while the corresponding hot and cold spot classifications are summarized in Table 1.

Table 1. Emerging hot and cold spots results.

Hot/Cold Spot Pattern	Category Definitions	Summary of Results	
		PRUs	VRUs
New hotspot	The most recent time-step interval is hot for the first time.	3	3
Consecutive hot spot	A single uninterrupted run of hot time-step intervals comprising less than 90% of all intervals	19	4
Intensifying hot spot	At least 90% of the time-step intervals are hot, and becoming hotter over time	65	48
Persistent hot spot	At least 90% of the time-step intervals are hot, with no trend up or down	29	28

Table 1. *Cont.*

Hot/Cold Spot Pattern	Category Definitions	Summary of Results	
		PRUs	VRUs
Diminishing hot spot	At least 90% of the time-step intervals are hot, and becoming less hot over time	2	6
Sporadic hot spot	Some of the time-step intervals are hot	35	2
Oscillating hot spot	Some of the time-step intervals are hot, some are cold	22	0
Historical hot spot	At least 90% of the time-step intervals are hot, but the most recent time-step interval is not	0	1
New cold spot	The most recent time-step interval is cold for the first time.	11	8
Consecutive cold spot	A single uninterrupted run of cold time-step intervals, comprising less than 90% of all intervals	98	79
Intensifying cold spot	At least 90% of the time-step intervals are cold, and becoming colder over time	105	3
Persistent cold spot	At least 90% of the time-step intervals are cold, with no trend up or down	0	47
Diminishing cold spot	At least 90% of the time-step intervals are cold, and becoming less cold over time	0	0
Sporadic cold spot	Some of the time-step intervals are cold	3	7
Oscillating cold spot	Some of the time-step intervals are cold, some are hot	4	0
Historical cold spot	At least 90% of the time-step intervals are cold, but the most recent time-step interval is not	0	0
No pattern detected	Does not fall into any of the hot or cold spot patterns defined above	91	239

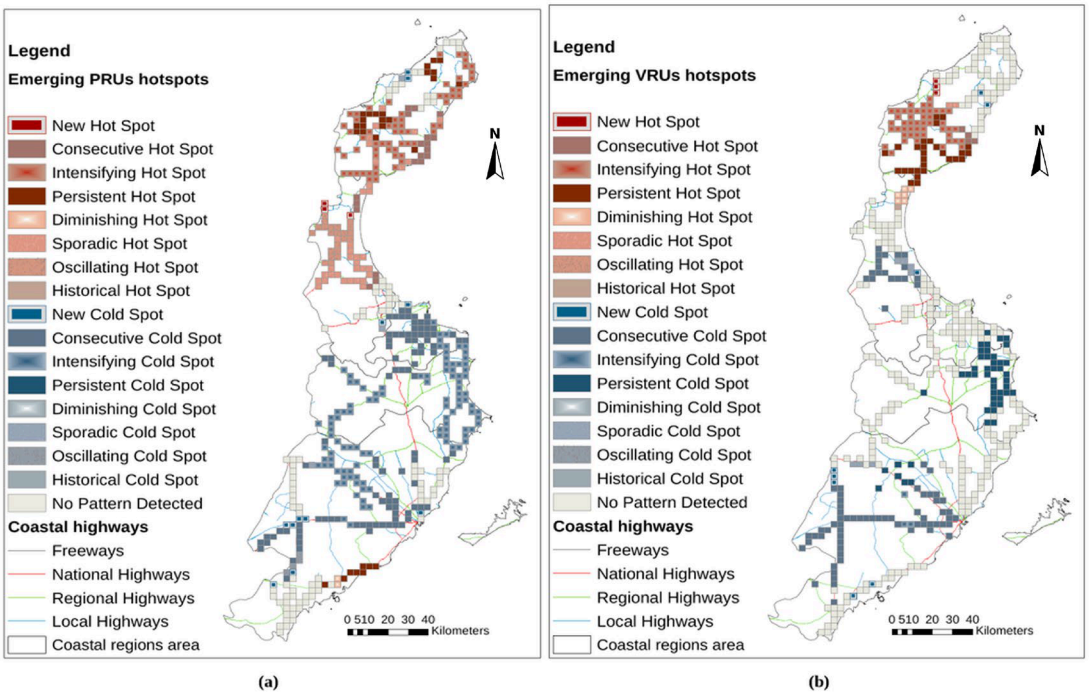

Figure 7. Emerging (**a**) PRU and (**b**) VRU hotspots.

For PRU collisions, the EHA identified three new hot spots and 11 new cold spots, 19 consecutive hot spots and 98 consecutive cold spots, 65 intensifying hot spots and 105 intensifying cold spots, 29 persistent hot spots, two diminishing hot spots, 35 sporadic hot spots and three sporadic cold spots, and 22 oscillating hot spots. No historical hot spots, persistent cold spots, diminishing cold spots, or historical cold spots were identified for PRUs. For VRU collisions, the EHA identified three new hot spots and eight new cold spots, four consecutive hot spots and 79 consecutive cold spots, 48 intensifying hot spots and three intensifying cold spots, 28 persistent hot spots and 47 persistent cold spots, six diminishing hot spots, two sporadic hot spots and seven sporadic cold spots, and one historical hot spot. No oscillating hot spots, persistent cold spots, diminishing cold spots, or historical cold spots were identified for VRUs. The analysis identified 91 PRU locations and 239 VRU locations for which no defined spatial-temporal pattern was detected. These locations were concentrated mainly in the central part of the study area, particularly in the Monastir and Mahdia governorates. Figure 8 presents a fine-scale geospatial view of the most critical PRU and VRU emerging hotspot locations. For PRUs, three new hot spots were identified, with these locations occurring mainly at the entrances and exits between the Nabeul and Sousse regions. For VRUs, the new hot spots were concentrated mainly in the Nabeul region, particularly in the northwestern part of the study area and around the road junction between RH-26 and LH-583. A total of 19 consecutive hot spots for PRUs and four consecutive hot spots for VRUs were identified. These locations were concentrated mainly on the eastern outskirts of the Nabeul region. The analysis also identified 29 persistent hot spots for PRUs and 28 persistent hot spots for VRUs. These locations were concentrated mainly in the Nabeul region, including areas on the western outskirts and around the city center. A total of 65 intensifying hot spots for PRUs and 48 intensifying hotspots for VRUs were identified. These locations correspond to areas in which the intensity of clustering increased over time and where statistically significant hot spots occurred during at least 90% of the time-step intervals, including the final time step.

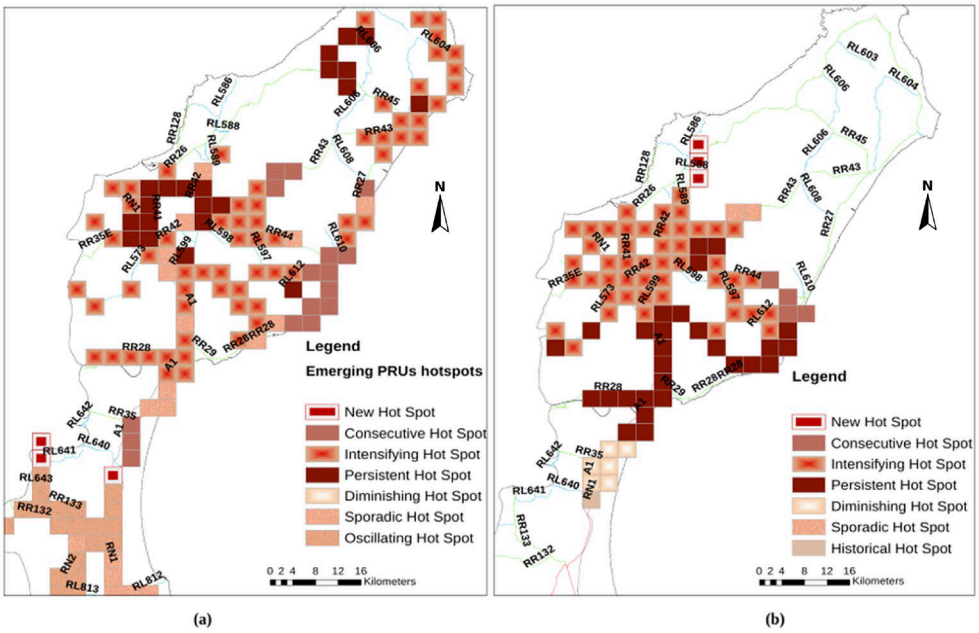

Figure 8. Fine-scale geospatial view of most critical (**a**) PRU and (**b**) VRU emerging hotspots.

The EHA identified 35 sporadic hot spots for PRUs and two for VRUs. PRU sporadic hot spots were concentrated mainly along RH-28 and RH-36, whereas VRU sporadic hotspots were concentrated mainly along RH-43. 22 oscillating hotspots were identified for PRUs,

whereas no oscillating hot spots were identified for VRUs. The PRU oscillating hotspots correspond to locations that were classified as statistically significant hotspots during the final time-step interval and had previously been classified as statistically significant cold spots during an earlier time step. Across the five-year study period, relatively few PRU and VRU emerging hotspots were identified on local highways compared with national and regional highways. Approximately 63% of the PRU emerging hotspots and 90% of the VRU emerging hot spots were located in the Nabeul region.

5.4. Spatio-Temporal Pattern of PRU and VRU Hotspots

To capture temporal heterogeneity in spatial crash dynamics, the Average Nearest Neighbor analysis (ANN) was run in ArcGIS 10.6 to assess how clustered or dispersed locations of PRU and VRU collisions disaggregated by hourly intervals and weekly periods. The ANN tool measures the distance between each feature centroid and its nearest neighbor's centroid location. The ANN ratio is given as:

$$\text{ANN} = \frac{D_{\text{Obs}}}{D_{\text{Exp}}} \tag{8}$$

$$D_{\text{Obs}} = \frac{\sum_{i=1}^{n} d_i}{n} \tag{9}$$

$$D_{\text{Exp}} = \frac{0.5}{\sqrt{\frac{N}{S}}} \tag{10}$$

where D_{Obs} is the observed mean distance between each feature and their nearest neighbor, D_{Exp} is the expected mean distance for the features given a random pattern, d_i is the distance between feature i and its nearest feature, N is the total number of features and S corresponds to the total study area. The z-score for the ANN statistic is given as:

$$Z_{\text{ANN-score}} = \frac{D_{\text{Obs}} - D_{\text{Exp}}}{SE_D} \tag{11}$$

$$SE_D = \frac{0.26136}{\sqrt{\frac{N^2}{S}}} \tag{12}$$

where SE_D is the standard error of the mean nearest neighbor distances.

Results of bivariate ANN conditioned by the hour of day and day of the week are presented in Table 2.

For PRUs, all eight temporal conditions produced statistically significant clustered patterns, with ANN ratios below 1 and p-values < 0.001. On working days, the ANN ratios were 0.36 for the morning peak, 0.22 for midday, 0.22 for the evening peak, and 0.32 for the night period. The corresponding ZANN-scores were −24.75, −42.77, −46.22, and −31.64, respectively. For weekend days, the ANN ratios were 0.67, 0.30, 0.38, and 0.27 for the morning peak, midday, evening peak, and night periods, respectively, with ZANN-scores of −7.82, −25.94, −17.63, and −32.48.

For VRUs, all eight temporal conditions also produced statistically significant clustered patterns, with ANN ratios below 1 and p-values < 0.001. On working days, the ANN ratios were 0.32 for the morning peak, 0.18 for midday, 0.24 for the evening peak, and 0.25 for the night period. The corresponding ZANN-scores were −22.15, −45.65, −41.05, and −35.79, respectively. For weekend days, the ANN ratios were 0.79, 0.34, 0.37, and 0.31 for the morning peak, midday, evening peak, and night periods, respectively, with ZANN-scores of −3.37, −22.11, −16.78, and −27.29.

Table 2. Bivariate ANN conditioned by hour of day and day of the week.

Road Users' Category	Sub-Time Periods	ANN	Z_{ANN}-Score	*p*-Value	Level of Aggregation	The Null Hypothesis of Randomness
PRUs						
Working days	A.M. peak (06:00–08:59)	0.36	−24.75	0.000	Clustered	Rejected
	Midday (09:00–16:59)	0.22	−42.77	0.000	Clustered	Rejected
	P.M. peak (17:00–19:59)	0.22	−46.22	0.000	Clustered	Rejected
	Night (20:00–05:59)	0.32	−31.64	0.000	Clustered	Rejected
Weekend days	A.M. peak (06:00–08:59)	0.67	−7.82	0.000	Clustered	Rejected
	Midday (09:00–16:59)	0.30	−25.94	0.000	Clustered	Rejected
	P.M. peak (17:00–19:59)	0.38	−17.63	0.000	Clustered	Rejected
	Night (20:00–05:59)	0.27	−32.48	0.000	Clustered	Rejected
VRUs						
Working days	A.M. peak (06:00–08:59)	0.32	−22.15	0.000	Clustered	Rejected
	Midday (09:00–16:59)	0.18	−45.65	0.000	Clustered	Rejected
	P.M. peak (17:00–19:59)	0.24	−41.05	0.000	Clustered	Rejected
	Night (20:00–05:59)	0.25	−35.79	0.000	Clustered	Rejected
Weekend days	A.M. peak (06:00–08:59)	0.79	−3.37	0.000	Clustered	Rejected
	Midday (09:00–16:59)	0.34	−22.11	0.000	Clustered	Rejected
	P.M. peak (17:00–19:59)	0.37	−16.78	0.000	Clustered	Rejected
	Night (20:00–05:59)	0.31	−27.29	0.000	Clustered	Rejected

Overall, the ANN results indicate statistically significant spatial clustering of both PRU and VRU collision locations across all examined combinations of day type and time period. The lowest ANN ratio for PRUs was observed during midday and the evening peak on working days (0.22 in both periods), whereas the lowest ANN ratio for VRUs was observed during midday on working days (0.18). The highest ANN ratios were observed during the weekend morning peak for both PRUs (0.67) and VRUs (0.79).

The bivariate co-maps presented in Figures 9 and 10 provide the spatial distribution of collision concentrations by time period for PRUs and VRUs, respectively. Figure 9 presents the PRU collision patterns, while Figure 10 presents the corresponding VRU patterns.

The co-maps show collision concentrations across the four temporal periods for both working days and weekend days. For both PRUs and VRUs, collision concentrations are observed during the morning peak (06:00–08:59), midday (09:00–16:59), evening peak (17:00–19:59), and night (20:00–05:59). The spatial patterns differ in their concentration and geographic distribution across the temporal periods.

The working-day co-maps show more pronounced spatial concentrations across the examined periods, whereas collision concentrations are also present during weekend periods. The figures further show areas where PRU and VRU collision concentrations occur within similar temporal windows as well as areas where their spatial patterns differ.

Taken together, the bivariate ANN results and co-maps demonstrate that PRU and VRU collision locations were significantly clustered across all examined temporal periods. The results also show both common and distinct spatial patterns between PRUs and VRUs across working days, weekends, and different periods of the day.

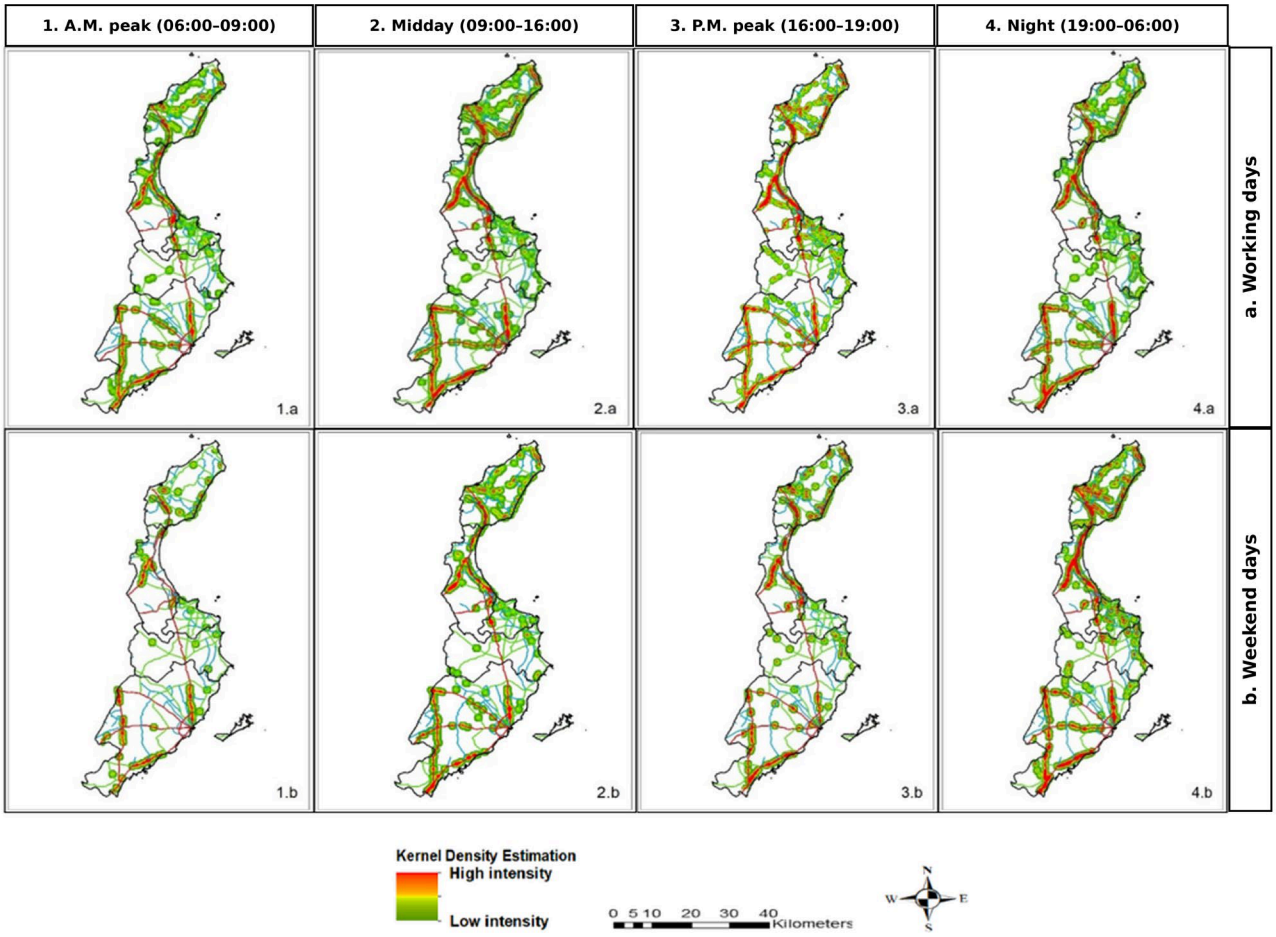

Figure 9. Bivariate co-map for PRU collisions (by hour and days of the week).

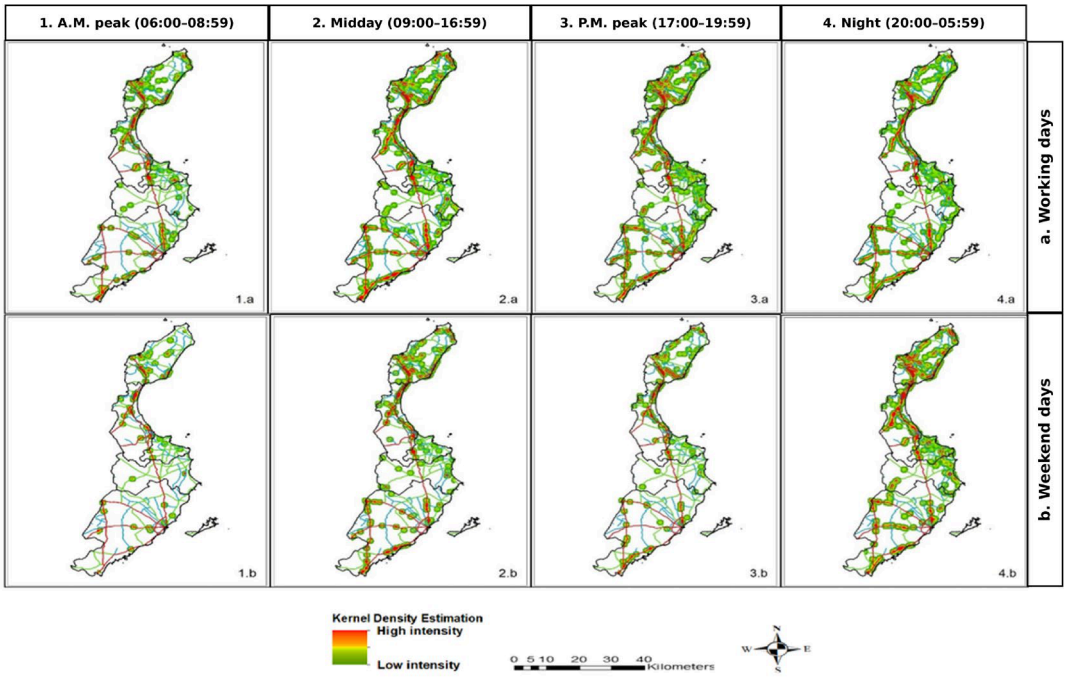

Figure 10. Bivariate co-map for VRU collisions (by hour and days of the week).

6. Discussion

The findings demonstrate that collision concentrations involving protected road users (PRUs) and vulnerable road users (VRUs) are structured across both temporal and spatial dimensions rather than being randomly distributed across the Tunisian coastal road network. The temporal analysis revealed distinct but partially overlapping patterns between the two groups. PRU collisions exhibited greater temporal fluctuations across the study period, whereas VRU collisions showed a comparatively more even distribution. This difference indicates that the temporal pattern of collision occurrence varies between road-user groups and supports the importance of differentiating PRUs and VRUs rather than analyzing all road users as a single population. Previous research has similarly demonstrated that road traffic collisions vary according to the time of day, day of week, and seasonal or annual conditions, confirming the value of incorporating multiple temporal dimensions into road-safety analysis [8,9,12]. The reduction in collision occurrences observed during 2020 represents an important discontinuity in the five-year series. The timing of this reduction coincides with the exceptional disruption of normal mobility patterns associated with the COVID-19 period. Restrictions on movement, changes in commuting behavior, reductions in travel activity, and temporary changes in the use of transport infrastructure may have influenced the observed collision distribution. However, the present study does not include direct traffic-volume or mobility-exposure measures, and therefore the specific contribution of these mechanisms cannot be quantified. The 2020 reduction should consequently be interpreted as a contextual feature of the collision series rather than as evidence of a direct causal effect.

The intra-day results further demonstrate differences between PRUs and VRUs. PRU collisions and injuries were more concentrated during weekday morning and evening periods, broadly corresponding to the main daily mobility periods. This pattern is consistent with the possibility that commuting and work-related travel contribute to the temporal concentration of collisions involving motorized road users. Previous research has documented significant variation in crash occurrence across different times of the day and days of the week, including differences between daytime, nighttime, and other temporal periods [8,9,12]. Similarly, ref. [58] identified an important relationship between rush-hour periods and fatal and non-fatal crash injuries. Nevertheless, because the present study does not contain direct measures of traffic exposure, travel demand, or road-user activity by the time of day, greater traffic exposure cannot be established as the direct cause of the observed concentrations.

For VRUs, collisions and injuries were predominantly distributed during daytime periods, particularly during the mid-morning and late-afternoon intervals. This pattern may reflect the temporal organization of pedestrian, cyclist, and motorcyclist activity, although direct measures of VRU exposure were not available. The distinction between the temporal profiles of PRUs and VRUs is therefore important from an analytical perspective. Previous research has emphasized that vulnerable road users may experience different exposure and injury conditions from motorized road users because they lack the physical protection provided by a vehicle [14]. The present findings extend this perspective by demonstrating that the temporal distribution of reported collisions also differs between the two groups.

The distribution of fatalities also differs from that of total collision and injury occurrences. For PRUs, fatalities were more dispersed across the temporal matrix, whereas VRU fatalities showed greater concentration during late-night periods and weekends. These patterns may be associated with contextual factors such as visibility, vehicle speed, road-user behavior, and characteristics of the surrounding traffic environment. However, these factors were not directly measured in the present dataset. They should therefore be regarded as plausible explanations rather than empirically demonstrated causal mechanisms. This dis-

tinction is particularly relevant for VRUs because the absence of external physical protection can increase the consequences of a collision [14].

The spatial findings reveal substantial heterogeneity across the study area, with statistically significant PRU and VRU hotspots concentrated primarily in the northern part of the coastal region, particularly in Nabeul and Sousse. This concentration indicates that reported collision locations are not spatially random and that particular road corridors and locations account for a disproportionate share of the observed collision concentration. Similar research has demonstrated the value of spatial statistical approaches for identifying non-random collision concentrations and distinguishing localized clusters from the broader distribution of crashes [54,59]. However, the identified hotspots should be interpreted as areas of elevated collision concentration rather than direct measures of exposure-adjusted crash risk, because the present analysis does not incorporate traffic volume, road-user exposure, population exposure, or other denominator-based measures.

The concentration of hotspots along major national and regional highways may reflect the interaction between the structure of the road network and the mobility functions of these corridors. The coastal region contains major population centers and important economic, commercial, tourism, and transport activities, and the road network consequently accommodates different forms of mobility. Research examining the relationship between traffic accidents, road-network configuration, and urban land use has similarly demonstrated that spatial collision patterns can be associated with the configuration of the transport network and surrounding land-use characteristics [59]. In the present study, however, such relationships were not directly modeled. The concentration of collisions along particular highways may therefore reflect a combination of traffic exposure, network connectivity, local mobility demand, land-use characteristics, and other contextual factors that require additional data to disentangle.

The fine-scale hotspot results are particularly relevant around major road junctions and intersections. The concentration of PRU and VRU hotspots around locations such as the intersections of NH1 with RH28 and RH42 suggests that complex connectivity nodes are important locations within the observed collision distribution. This finding is consistent with those of previous studies showing that road intersections and transitions between different road classifications can represent important collision-concentration locations [54,60,61]. However, the present analysis identifies spatial concentrations but does not directly test whether intersection geometry, signalization, traffic conflicts, road design, or pedestrian facilities are responsible for the observed hotspots.

The concentration of hotspots in Nabeul and Sousse should also be considered in relation to the broader socio-spatial structure of the study area. The manuscript identifies these areas as important population and mobility centers, while the coastal region as a whole contains substantial economic and transport activity. Consequently, higher collision counts may partly reflect higher levels of mobility and exposure. This interpretation reinforces the distinction between collision concentration and crash risk. A location with a high number of reported collisions is not necessarily a location with a higher individual risk if the corresponding traffic or road-user exposure is also substantially higher.

The spatial differences between PRUs and VRUs provide further evidence that the two road-user groups should not be treated as a single analytical population. Although both groups exhibit substantial hotspot concentrations in Nabeul and Sousse, their spatial patterns are not identical. The PRU hotspot pattern is more broadly distributed across several major road corridors, whereas some VRU hotspot categories show more localized concentrations around particular areas and junctions. These differences may reflect variation in mobility patterns, road-user activity, and the environments in which protected and vulnerable users interact. Previous research has similarly emphasized that VRU exposure

and injury conditions can differ substantially across dense and heterogeneous road environments [14]. In the present study, however, detailed pedestrian, cyclist, and motorcyclist exposure data were not available, and therefore the mechanisms underlying these spatial differences cannot be directly established.

The emerging hotspot analysis adds an important temporal dimension to the static spatial hotspot results. Rather than simply identifying where collision concentrations occur, the analysis distinguishes locations according to how their hotspot status changes across the five-year period. This provides a more differentiated interpretation of the spatial patterns because a hotspot that is persistent, intensifying, sporadic, or newly emerging does not have the same temporal meaning. The use of space-time cube and emerging hotspot analysis is consistent with previous applications demonstrating that the combination of spatial clustering and temporal trend analysis can reveal changes that are not visible in a conventional two-dimensional hotspot map [6,8,12,40–43,58,62,63]. Studies using space-time cube and emerging hotspot analysis have identified persistent, intensifying, emerging, and sporadic patterns across different road environments, including urban areas, major freight corridors, and national road networks [6,8,40–43,58,62,63].

The identification of new hotspots for both PRUs and VRUs indicates that a limited number of locations developed statistically significant hotspot characteristics during the study period. The PRU new hotspots were mainly located around entrances and exits between the Nabeul and Sousse areas, whereas VRU new hotspots were concentrated mainly in the Nabeul region, including the area around the RH-26 and LH-583 junction. The concentration of new hotspots around city entrances and exits is consistent with the previous research showing that important crash concentration areas can occur around city entrances and urban centers [64]. In the present study, the association between new hotspots and commercial or mobility activity around these locations is a plausible interpretation, but it was not directly tested using land-use or traffic-activity data.

The persistent and intensifying hotspot categories are particularly important because they indicate that some locations repeatedly exhibit statistically significant clustering or increasing hotspot intensity over the study period. The concentration of persistent hotspots in Nabeul, including areas around the western outskirts and the city center, suggests that some collision concentrations are not temporary phenomena but remain present across multiple time intervals. Similarly, the identification of intensifying hotspots indicates locations where the intensity of high collision counts increased over time and where statistically significant hotspot conditions were observed during most of the time-step intervals, including the final interval. These patterns provide information that cannot be obtained from a single static hotspot map. They are also consistent with the broader literature demonstrating that temporal hotspot analysis can distinguish stable concentrations from locations undergoing changes in collision patterns [6,8,40–43,58,62,63].

The distribution of sporadic hotspots provides a complementary finding. PRU sporadic hotspots were concentrated mainly along RH-28 and RH-36, while VRU sporadic hotspots were mainly associated with RH-43. The concentration of PRU sporadic hotspots along RH-28 is noteworthy because this corridor connects several important roadways, including NH1, the A1 motorway, RH-35, and LH-625. Such connectivity may contribute to variable traffic conditions and changing collision concentrations over time. However, the present study does not contain the traffic-flow data necessary to test this explanation directly. More generally, the research on spatial clustering of events on transport networks has shown that the configuration of the underlying network can influence the spatial organization of events [65]. Therefore, the observed differences between national, regional, and local highways should be interpreted in relation to network structure and exposure rather than simply as evidence that one road class is intrinsically safer than another.

The relatively high proportion of emerging hotspots located in Nabeul further reinforces the spatial concentration identified by the optimized hotspot analysis. Approximately 63% of PRU emerging hotspots and 90% of VRU emerging hotspots were located in Nabeul. The consistency between the optimized hotspot results and the emerging hotspot results suggests that Nabeul is not only characterized by a high concentration of reported collisions but also contains locations where hotspot patterns exhibit meaningful temporal dynamics. Nevertheless, these results should not be interpreted as evidence that Nabeul has intrinsically higher crash risk because exposure-adjusted measures were not available.

The bivariate Average Nearest Neighbor analysis and co-mapping further demonstrate that the spatial organization of collisions changes according to the time of day and day of week. Both PRUs and VRUs exhibited statistically significant spatial clustering across all examined combinations of working days, weekends, and time periods. The strongest clustering occurred during several daytime and evening periods, particularly on working days, while weekend patterns were generally less concentrated in some temporal periods. This finding is consistent with previous evidence that collision clustering can vary across temporal scales, including time of day, day of week, and seasonal or special-period conditions [8]. It also complements the temporal heatmap results by demonstrating that temporal variation is not simply a change in the number of collisions; the spatial arrangement of collision locations also changes according to temporal context.

An important finding from the bivariate co-maps is the existence of both converging and diverging spatial patterns between PRUs and VRUs. Some locations and temporal periods show concentrations for both groups, indicating shared spatial and temporal environments, whereas other locations display more distinct patterns. This finding is consistent with the conceptual distinction between protected and vulnerable road users. PRUs and VRUs operate within the same transportation system but do not experience that system under identical conditions. The previous research has shown that VRUs may be particularly affected by interactions with motorized traffic, intersections, mixed-traffic environments, and the absence of physical protection [14]. The present findings support the need to distinguish the two groups analytically while recognizing that their collision patterns can overlap in common transport environments.

The temporal convergence between PRUs and VRUs during important mobility periods is particularly relevant. The bivariate results indicate that both groups exhibit substantial collision concentrations during midday, evening, and night periods, although the strength and geographical distribution of these concentrations differ. The research on rush-hour periods has demonstrated that temporal periods of increased mobility can be associated with changes in fatal and non-fatal crash injuries [58]. In the present study, however, it would be inappropriate to attribute the observed concentrations exclusively to traffic volume, fatigue, visibility, or behavioral factors because these variables were not directly measured. Instead, the results indicate that particular temporal windows repeatedly coincide with spatially clustered collision locations.

Taken together, the findings demonstrate that the spatial and temporal dimensions of road traffic collisions are closely interconnected. The temporal heatmaps identify when collision concentrations occur; the optimized hotspot analysis identifies where statistically significant spatial concentrations occur; the emerging hotspot analysis shows how these concentrations evolve over time; and the bivariate Average Nearest Neighbor and co-mapping analyses demonstrate how spatial patterns vary across specific temporal contexts and between PRUs and VRUs. The integration of these complementary approaches therefore provides a more complete description of collision concentration patterns than any single analytical method alone. This is consistent with the broader literature showing the value of integrating spatial and temporal approaches in road-safety analysis [6,8,9,12,40–43,58,62,63].

Overall, the findings indicate that PRU and VRU collision concentrations in Tunisia's coastal regions are characterized by substantial spatial heterogeneity, temporal variation, and evolving hotspot dynamics. The northern concentration of hotspots, the repeated identification of Nabeul as an important area of emerging and persistent patterns, the concentration around major corridors and junctions, and the temporal differences and overlaps between PRUs and VRUs demonstrate that collision concentrations are dynamic rather than spatially or temporally uniform. At the same time, the findings should be interpreted within the limitations of the available data. The analyses are based on police-reported fatal and injury-related collisions and do not include comprehensive measures of traffic exposure, pedestrian or cyclist activity, road characteristics, land use, weather, lighting, road-surface conditions [66], vehicle speed, or other contextual variables. Consequently, the observed hotspot concentrations may partly reflect differences in exposure rather than disproportionately elevated crash risk. The spatial and temporal associations identified in this study should therefore not be interpreted as causal relationships.

7. Theoretical and Practical Implications

This study advances the field of road safety analysis by introducing an integrated, multi-stage geospatial analytical framework that combines optimized hotspot analysis, space–time pattern mining framework using emerging hotspot analysis, bivariate co-mapping clustering, and multi-temporal scale analysis to investigate the spatio-temporal dynamics of PRU and VRU collision hotspots.

By moving beyond conventional static mapping approaches, this research captures both the spatial concentration and temporal evolution of risk across heterogeneous user groups, thereby offering a more comprehensive and dynamic understanding of collision processes. The methodological novelty lies in the synergistic use of machine-learning-based pattern recognition and advanced cartographic analysis to detect optimized and emerging hotspots, enabling a fine-grained interpretation of how exposure patterns, mobility behaviors, and infrastructural configurations interact over time. This integrated approach represents a robust analytical template for future studies seeking to model complex transport-related risk phenomena under conditions of rapid urban and mobility transformation. A key theoretical contribution of this work is the explicit differentiation between VRUs and PRUs, which reveals distinctive spatial distributions, temporal rhythms, and risk intensities that would remain obscured under aggregated analyses. Moreover, the clear identification of interday variability (weekdays vs. weekends) and intra-day temporal differentials underscore the necessity of incorporating a fine-grained spatio-temporal dimension into predictive safety planning models. These temporal asymmetries reveal continuously evolving exposure patterns and interaction frequencies, illustrating that collision risk is inherently dynamic and governed by recurring mobility rhythms, land-use configurations, and temporal behavioral adaptations. Integrating such temporal granularity into risk modeling frameworks is therefore critical for accurately representing the evolving patterns of vulnerability and for guiding time-sensitive and context-specific intervention strategies.

8. Conclusions and Future Research Directions

This research examined the spatial and spatio-temporal characteristics of collision hotspots involving vulnerable road users (VRUs) and protected road users (PRUs) across Tunisia's coastal regions. The study pursued three main objectives: (1) to map collision distributions and identify spatial clustering patterns for the two road-user groups; (2) to examine temporal variations in collision patterns across different hours, days, and years; and (3) to integrate spatial and temporal information to characterize the evolution and geographic overlap of collision hotspots. Using five years of georeferenced collision records

(2018–2022), comprising 4090 PRU and 3600 VRU incidents across approximately 3720 km of coastal roads, the analysis combined optimized hotspot analysis (OHA), emerging hotspot analysis (EHA) based on the space-time cube, Kernel Density Estimation (KDE), and bivariate co-mapping.

The findings reveal a heterogeneous spatial distribution of collisions, with notable concentrations in northern coastal areas, particularly in the Nabeul region. The results of the hotspot analyses indicate that collision concentrations differ between PRUs and VRUs, demonstrating the importance of examining these road-user groups separately rather than relying exclusively on aggregated collision patterns. Emerging hotspot analysis further identified different temporal hotspot classifications. In particular, 65 intensifying hotspots were identified for PRUs and 48 for VRUs, while 35 PRU and two VRU sporadic hotspots were detected. In addition, 22 oscillating hotspots were identified among PRUs. Approximately 63% of the emerging PRU hotspots and 90% of the emerging VRU hotspots were located in the Nabeul region. These findings highlight the geographical concentration of collision hotspots and the importance of examining how their intensity and persistence vary over time. The temporal analyses also identified recurring patterns of collision clustering across different periods of the day and week. Both PRUs and VRUs exhibited clustered spatial distributions during morning peak hours, midday, evening peak hours, and nighttime, on both working days and weekends. The bivariate co-mapping results indicated shared temporal patterns between the two groups, particularly during midday and evening periods, while also revealing differences in the distribution and intensity of their collision concentrations.

The contribution of this study lies in its integrated empirical assessment of PRU and VRU collision patterns across Tunisia's coastal regions through the combined application of established spatial and spatio-temporal analytical techniques. By examining spatial concentration, temporal variation, emerging hotspot classifications, and geographic overlap separately for the two road-user groups, the study provides a differentiated characterization of collision patterns within a common analytical framework. Rather than introducing new GIS algorithms, this research demonstrates the value of applying complementary methods to examine road-safety patterns from multiple spatial and temporal perspectives. The results provide a basis for identifying locations and periods that may warrant further investigation by road-safety authorities and for informing the development of context-specific prevention strategies.

Limitations and Future Research Directions

This study has several limitations that should guide the interpretation of its findings and future refinement of the framework. First, the hotspot analyses are based primarily on collision counts and spatial density and do not account for exposure factors such as traffic volume, road length, population density, land use, or pedestrian and cyclist activity. Consequently, hotspots may partly reflect higher exposure rather than disproportionately higher collision risk. The identified hotspots should therefore be interpreted as areas of elevated collision concentration rather than direct measures of exposure-adjusted risk. Future research should incorporate appropriate exposure measures, such as normalization factors or covariates in exposure-adjusted risk models, to better distinguish high collision frequency from disproportionately high risk. This distinction is reinforced by recent crash-severity modeling work that treats severity as a separate outcome predicted from explanatory variables such as road-user characteristics and contextual crash factors [67]; extending the present framework with a comparable severity-coded outcome, rather than relying on collision counts alone, represents a natural direction for future research.

Second, the analysis relies on police-reported collision records from NORS, which are subject to the underreporting typically associated with police-based road-safety data, particularly for minor VRU collisions.

Third, the spatial and temporal parameters used in the space-time cube (3169 m grid, one-year step) and Kernel Density Estimation (3000 m bandwidth, 1000 m cell size) were calibrated through exploratory testing rather than a full systematic sensitivity analysis. Because hotspot detection can be sensitive to the choice of spatial units and aggregation scale, an issue known as the Modifiable Areal Unit Problem (MAUP), the hotspot locations and counts reported in Section 5 should be interpreted as conditional on the selected spatial partition. Alternative spatial resolutions may produce different hotspot counts, locations, or classifications. Although the space-time cube resolution was established using ArcGIS's default sizing procedure, a systematic sensitivity analysis using alternative grid sizes was not conducted. Consequently, the stability of the identified hotspots across different spatial aggregation scales remains uncertain. Future studies should assess hotspot stability across a range of parameter settings.

Another limitation concerns the validation of the analytical framework. Although multiple spatial and spatio-temporal techniques were employed to characterize collision patterns, no formal cross-method agreement assessment or independent validation against an external dataset was conducted. Consequently, the combined application of OHA, EHA, KDE, and co-mapping should not be interpreted as independent confirmation of hotspot reliability or predictive performance. Future research should quantify the spatial agreement between hotspot classifications generated by different methods using harmonized spatial units and explicitly defined comparison criteria.

The analysis is also retrospective in nature. Although emerging hotspot analysis identifies historical patterns such as intensifying, persistent, and sporadic hotspots, these classifications do not constitute predictions of future collision occurrence. The study did not conduct out-of-sample testing or prospective evaluation of future collision locations or frequencies; therefore, the predictive performance of the framework has not been established. Future research could develop and evaluate predictive models using longer collision time series, appropriate exposure measures, and independent temporal or spatial test data. Such evaluation would help determine whether historical collision patterns can reliably inform forecasts of future collision locations or frequencies.

Finally, explanations for hotspot concentration, including speed, signage, lighting, and driving behavior, are plausible interpretations based on the previous literature but were not directly tested in the spatial models. Field investigations, such as site audits and speed surveys, are therefore recommended before implementing specific engineering countermeasures. Future research should also assess the transferability of the framework to other resource-constrained regions beyond the Tunisian coastal context.

Funding: This research received no external funding. The article processing charge was funded by Sharjah Maritime Academy's Research Support Scheme.

Institutional Review Board Statement: Not applicable.

Informed Consent Statement: Not applicable.

Data Availability Statement: The raw data supporting the conclusions of this article will be made available by the authors on request.

Acknowledgments: The author gratefully acknowledges the support of Sharjah Maritime Academy.

Conflicts of Interest: The author declares no conflicts of interest.

Appendix A

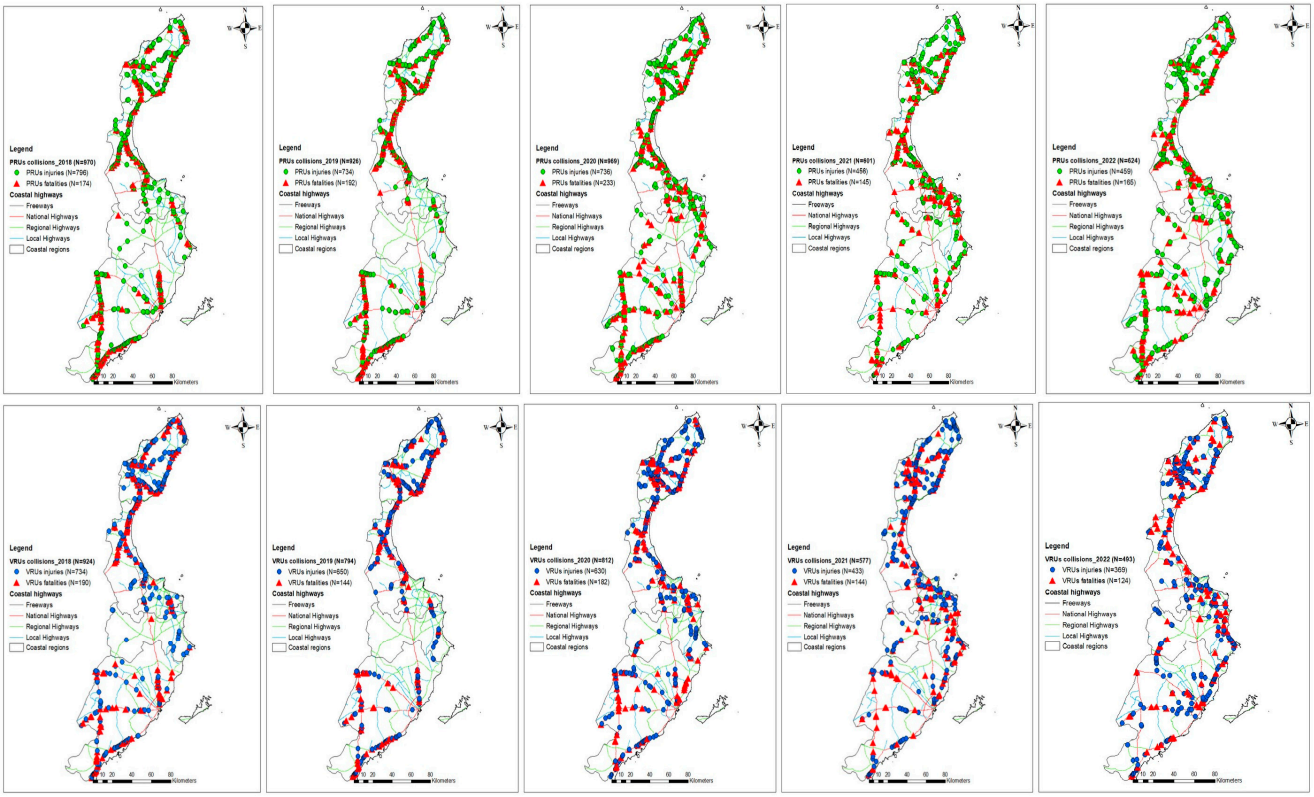

Figure A1. PRU and VRU collision distribution (2018–2022).

References

1. World Health Organization. *Global Status Report on Road Safety 2013: Supporting a Decade of Action*; World Health Organization: Geneva, Switzerland, 2013.
2. Aghajani, M.A.; Dezfoulian, R.S.; Arjroody, A.R.; Rezaei, M. Applying GIS to identify the spatial and temporal patterns of road accidents using spatial statistics (case study: Ilam Province, Iran). *Transp. Res. Procedia* **2017**, *25*, 2126–2138. [CrossRef]
3. Ouni, F.; Belloumi, M. Pattern of road traffic crash hot zones versus probable hot zones in Tunisia: A geospatial analysis. *Accid. Anal. Prev.* **2019**, *128*, 185–196. [CrossRef] [PubMed]
4. Moyer, J.D.; Eshbaugh, M.; Rettig, J. Cost analysis of global road traffic death prevention: Forecasts to 2050. *Dev. Policy Rev.* **2017**, *35*, 745–757. [CrossRef]
5. Damsere-Derry, J.; Palk, G.; King, M. Road accident fatality risks for "vulnerable" versus "protected" road users in northern Ghana. *Traffic Inj. Prev.* **2017**, *18*, 736–743. [CrossRef] [PubMed]
6. Wang, M.; Yi, J.; Chen, X.; Zhang, W.; Qiang, T. Spatial and Temporal Distribution Analysis of Traffic Accidents Using GIS-Based Data in Harbin. *J. Adv. Transp.* **2021**, *2021*, 9207500. [CrossRef]
7. Endashaw, D.K.; Habtegiorgis, K.A.; Al-Ramadan, B.M.; Al-Ahmadi, H.M.; Deressa, B.F. A systematic review on GIS-based road traffic accidents analysis and road safety audit. *Comput. Urban Sci.* **2025**, *5*, 53. [CrossRef]
8. Iamtrakul, P.; Chayphong, S. GIS-based analysis of spatio-temporal clustering of road traffic accidents in Bangkok Metropolitan Region (BMR), Thailand from 2012 to 2021. *Transp. Res. Interdiscip. Perspect.* **2025**, *31*, 101489. [CrossRef]
9. Alsahfi, T. Spatial and temporal analysis of road traffic accidents in major Californian cities using a geographic information system. *ISPRS Int. J. Geo-Inf.* **2024**, *13*, 157. [CrossRef]
10. Ouni, F.; Belloumi, M. Spatio-temporal pattern of vulnerable road user's collisions hot spots and related risk factors for injury severity in Tunisia. *Transp. Res. Part F Traffic Psychol. Behav.* **2018**, *56*, 477–495. [CrossRef]
11. Ngozi, E.J.; Nkechiis, B.C.; Abdulwaheed, Y.M. Mapping and Analysis of the Temporal Changes of Road Traffic Accident Hotspots Using GIS and Remote Sensing in Owerri, Imo State, Nigeria. *Int. J. Innov. Res. Dev.* **2021**, *10*, 128–140. [CrossRef]
12. Kang, Y.; Cho, N.; Son, S. Spatiotemporal characteristics of elderly population's traffic accidents in Seoul using space-time cube and space-time kernel density estimation. *PLoS ONE* **2018**, *13*, e0196845. [CrossRef] [PubMed]

13. Kalantari, M.; Zanganeh Shahraki, S.; Yaghmaei, B.; Ghezelbash, S.; Ladaga, G.; Salvati, L. Unraveling urban form and collision risk: The spatial distribution of traffic accidents in Zanjan, Iran. *Int. J. Environ. Res. Public Health* **2021**, *18*, 4498. [CrossRef] [PubMed]
14. Campolettano, E.T.; Scanlon, J.M.; Kadar, I.; Lavy, L.Y.; Moura, D.C.; Kusano, K.D. Baseline vulnerable road user injury risk in multiple US dense urban driving environments. *Traffic Inj. Prev.* **2024**, *25*, S94–S104. [CrossRef] [PubMed]
15. Karamanlis, I.; Nikiforiadis, A.; Botzoris, G.; Kokkalis, A.; Basbas, S. Towards Sustainable Transportation: The Role of Black Spot Analysis in Improving Road Safety. *Sustainability* **2023**, *15*, 14478. [CrossRef]
16. Al-Aamri, A.K.; Hornby, G.; Zhang, L.C.; Al-Maniri, A.A.; Padmadas, S.S. Mapping road traffic crash hotspots using GIS-based methods: A case study of Muscat Governorate in the Sultanate of Oman. *Spat. Stat.* **2021**, *42*, 100458. [CrossRef]
17. Flahaut, B.; Mouchart, M.; San Martin, E.; Thomas, I. The local spatial autocorrelation and the kernel method for identifying black zones: A comparative approach. *Accid. Anal. Prev.* **2003**, *35*, 991–1004. [CrossRef] [PubMed]
18. Elvik, R. A survey of operational definitions of hazardous road locations in some European countries. *Accid. Anal. Prev.* **2008**, *40*, 1830–1835. [CrossRef] [PubMed]
19. Lai, P.C.; Chan, W.Y. GIS for road accident analysis in Hong Kong. *Geogr. Inf. Sci.* **2004**, *10*, 58–67. [CrossRef]
20. Harirforoush, H.; Bellalite, L. A new integrated GIS-based analysis to detect hotspots: A case study of the city of Sherbrooke. *Accid. Anal. Prev.* **2019**, *130*, 62–74. [CrossRef] [PubMed]
21. Loo, B.P.; Yao, S. The identification of traffic crash hot zones under the link-attribute and event-based approaches in a network-constrained environment. *Comput. Environ. Urban Syst.* **2013**, *41*, 249–261. [CrossRef]
22. Hazaymeh, K.; Almagbile, A.; Alomari, A.H. Spatiotemporal analysis of traffic accidents hotspots based on geospatial techniques. *ISPRS Int. J. Geo-Inf.* **2022**, *11*, 260. [CrossRef]
23. Zheng, M.; Xie, X.; Jiang, Y.; Shen, Q.; Geng, X.; Zhao, L.; Jia, F. Optimizing Kernel Density Estimation Bandwidth for Road Traffic Accident Hazard Identification: A Case Study of the City of London. *Sustainability* **2024**, *16*, 6969. [CrossRef]
24. Gedamu, W.T.; Plank-Wiedenbeck, U.; Wodajo, B.T. A spatial autocorrelation analysis of road traffic crash by severity using Moran's I spatial statistics: A comparative study of Addis Ababa and Berlin cities. *Accid. Anal. Prev.* **2024**, *200*, 107535. [CrossRef] [PubMed]
25. Mahato, R.K.; Htike, K.M.; Sornlorm, K.; Koro, A.B.; Kafle, A.; Sharma, V. A spatial autocorrelation analysis of road traffic accidents by severity using Moran's I spatial statistics: A study from Nepal 2019–2022. *BMC Public Health* **2024**, *24*, 3086. [CrossRef] [PubMed]
26. Alam, M.S.; Tabassum, N.J. Spatial pattern identification and crash severity analysis of road traffic crash hot spots in Ohio. *Heliyon* **2023**, *9*, e16303. [CrossRef] [PubMed]
27. Soltani, A.; Askari, S. Exploring spatial autocorrelation of traffic crashes based on severity. *Injury* **2017**, *48*, 637–647. [CrossRef] [PubMed]
28. Ha, L.T.; Thao, V.T.P.; Thao, D.T.P. Analyzing Road Traffic Incident Hotspots Using Cluster Analysis in Thanh Hoa Province of Vietnam. *Int. J. Geoinformatics* **2024**, *20*, 16–26. [CrossRef]
29. Zou, Y.; Dong, C.; Shi, J. Spatio-temporal distribution characterization and blackspots identification of e-bike accidents: Based on accident dataset. *J. Transp. Saf. Secur.* **2025**, *17*, 1008–1026. [CrossRef]
30. Feizizadeh, B.; Omarzadeh, D. A GIS based spatiotemporal modelling approach for cycling risk mapping using crowd-sourced sensor data. *Ann. GIS* **2025**, *31*, 333–351. [CrossRef]
31. Cappelli, G.; Nardoianni, S.; D'Apuzzo, M.; Nicolosi, V. Cyclist Safety in Complex Urban Environments: Infrastructure, Traffic Interactions, and Spatial Anomalies in Rome, Italy. *Urban Sci.* **2026**, *10*, 73. [CrossRef]
32. Zhao, J.; Li, Z.; Liu, P.; Chen, K.; Zhai, X. Impact of road network patterns on traffic crash prediction: An interpretable geography machine learning approach. *J. Transp. Saf. Secur.* **2025**, *17*, 1319–1347. [CrossRef]
33. Kang, X.; Wu, D.; Sha, W.; Song, K.; Wang, S. Analysis and Prediction of Traffic Accidents Based on Interpretable Spatial Machine Learning: A Case Study in California. *J. Adv. Transp.* **2025**, *2025*, 3184284. [CrossRef]
34. Pourroostaei Ardakani, S.; Liang, X.; Mengistu, K.T.; So, R.S.; Wei, X.; He, B.; Cheshmehzangi, A. Road car accident prediction using a machine-learning-enabled data analysis. *Sustainability* **2023**, *15*, 5939. [CrossRef]
35. Shafay, M.; Anwar, H.N.; Bibi, I.; Samad, A.; Akhtar, N.; Rasheed, A.; Kazi, M.A. Seasonal and Time-Series Analysis of Road Traffic Accidents. *Pak. J. Health Sci.* **2024**, *5*, 121–125. [CrossRef]
36. Guerra, E.; Dong, X.; Lin, L.; Guo, Y. Temporal Analysis of Predictors of Pedestrian Crashes. *Transp. Res. Rec. J. Transp. Res. Board* **2020**, *2674*, 252–263. [CrossRef]
37. Weast, R. Temporal factors in motor-vehicle crash deaths: Ten years later. *J. Saf. Res.* **2018**, *65*, 125–131. [CrossRef] [PubMed]
38. Wiratama, B.S.; Chen, P.L.; Chen, L.H.; Saleh, W.; Chen, S.K.; Chen, H.T.; Lin, H.-A.; Pai, C.W. Evaluating the effects of holidays on road crash injuries in the United Kingdom. *Int. J. Environ. Res. Public Health* **2021**, *18*, 280. [CrossRef] [PubMed]
39. Harirforoush, H.; Bellalite, L.; Bénié, G.B. Spatial and temporal analysis of seasonal traffic accidents. *Am. J. Traffic Transp. Eng.* **2019**, *4*, 7–16. [CrossRef]

40. Mesic, A.; Damsere-Derry, J.; Feldacker, C.; Mooney, S.J.; Gyedu, A.; Mock, C.; Kitali, A.; Wagenaar, B.H.; Wuaku, D.H.; Afram, M.O.; et al. Identifying emerging hot spots of road traffic injury severity using spatiotemporal methods: Longitudinal analyses on major roads in Ghana from 2005 to 2020. *BMC Public Health* **2024**, *24*, 1609. [CrossRef] [PubMed]
41. Gudes, O.; Varhol, R.; Sun, Q.C.; Meuleners, L. Investigating articulated heavy-vehicle crashes in western Australia using a spatial approach. *Accid. Anal. Prev.* **2017**, *106*, 243–253. [CrossRef] [PubMed]
42. Mohammed, S.; Alkhereibi, A.H.; Abulibdeh, A.; Jawarneh, R.N.; Balakrishnan, P. GIS-based spatiotemporal analysis for road traffic crashes; in support of sustainable transportation planning. *Transp. Res. Interdiscip. Perspect.* **2023**, *20*, 100836. [CrossRef]
43. Younes, S.; Oloufa, A. A Geospatial Framework for Spatiotemporal Crash Hotspot Detection Using Space–Time Cube Modeling and Emerging Pattern Analysis. *Urban Sci.* **2025**, *9*, 411. [CrossRef]
44. Ouni, F.; Hzami, M.; Harizi, R. Spatio-temporal hotspots analysis of pedestrian-vehicle collisions in Tunisian coastal regions. In *Proceedings of the 2020 IEEE 13th International Colloquium of Logistics and Supply Chain Management (LOGISTIQUA), Fez, Morocco, 2–4 December 2020*; IEEE: Piscataway, NJ, USA, 2020; pp. 1–6. [CrossRef]
45. Fang, A.; Peng, X.; Zhou, J.; Tang, L. Research on the map-matching and spatial-temporal visualization of expressway traffic accident information. In *Proceedings of the 2018 3rd IEEE International Conference on Intelligent Transportation Engineering (ICITE), Singapore, 3–5 September 2018*; IEEE: Piscataway, NJ, USA, 2018; pp. 23–27. [CrossRef]
46. Silva, C.; Saraee, M. Predicting Road Traffic Accident Severity using Decision Trees and Time-Series Calendar Heatmaps. In *Proceedings of the 2019 IEEE Conference on Sustainable Utilization and Development in Engineering and Technologies (CSUDET), Penang, Malaysia, 7–9 November 2019*; IEEE: Piscataway, NJ, USA, 2019. [CrossRef]
47. ESRI—ArcGIS Pro. Optimized Hot Spot Analysis. 2021. Available online: https://pro.arcgis.com/fr/pro-app/latest/tool-reference/spatial-statistics/how-optimized-hot-spot-analysis-works.htm (accessed on 20 February 2021).
48. Abdulhafedh, A. A novel hybrid method for measuring the spatial autocorrelation of vehicular crashes: Combining Moran's Index and Getis-Ord Gi* statistic. *Open J. Civ. Eng.* **2017**, *7*, 208–221. [CrossRef]
49. Gundogdu, I.B. Applying linear analysis methods to GIS-supported procedures for preventing traffic accidents: Case study of Konya. *Saf. Sci.* **2010**, *48*, 763–769. [CrossRef]
50. Soltani, A.; Qadikolaei, M.R. Space-time analysis of accident frequency and the role of built environment in mitigation. *Transp. Policy* **2024**, *150*, 189–205. [CrossRef]
51. Brunsdon, C. The comap: Exploring spatial pattern via conditional distributions. *Comput. Environ. Urban Syst.* **2001**, *25*, 53–68. [CrossRef]
52. Plug, C.; Xia, J.C.; Caulfield, C. Spatial and temporal visualisation techniques for crash analysis. *Accid. Anal. Prev.* **2011**, *43*, 1937–1946. [CrossRef] [PubMed]
53. Choudhary, A.; Mishra, V.; Garg, R.D.; Jain, S.S. Spatio–temporal analysis of traffic crash hotspots—An application of GIS-based technique in road safety. *Appl. Geomat.* **2025**, *17*, 129–146. [CrossRef]
54. Le, K.G.; Liu, P.; Lin, L.-T. Determining the road traffic accident hotspots using GIS-based temporal-spatial statistical analytic techniques in Hanoi, Vietnam. *Geo-Spat. Inf. Sci.* **2019**, *23*, 153–164. [CrossRef]
55. Mohaymany, A.S.; Shahri, M.; Mirbagheri, B. GIS-based method for detecting high-crash-risk road segments using network kernel density estimation. *Geo-Spat. Inf. Sci.* **2013**, *16*, 113–119. [CrossRef]
56. Xie, Z.; Yan, J. Detecting traffic accident clusters with network kernel density estimation and local spatial statistics: An integrated approach. *J. Transp. Geogr.* **2013**, *31*, 64–71. [CrossRef]
57. Ge, H.; Dong, L.; Huang, M.; Zang, W.; Zhou, L. Adaptive Kernel Density Estimation for Traffic Accidents Based on Improved Bandwidth Research on Black Spot Identification Model. *Electronics* **2022**, *11*, 3604. [CrossRef]
58. Adeyemi, O.; Arif, A.; Paul, R. Exploring the Relationship of Rush Hour Period and Fatal and Non-Fatal Crash Injuries in the U.S.: A Systematic Review and Meta-Analysis. *Accid. Anal. Prev.* **2021**, *163*, 106462. [CrossRef] [PubMed]
59. Iranmanesh, A.; Kara, C.; Tülbentçi, T. Mapping the relationship between traffic accidents, road network configuration, and urban land use. *Int. J. Inj. Control Saf. Promot.* **2024**, *31*, 672–685. [CrossRef] [PubMed]
60. Cheng, Z.; Zu, Z.; Lu, J. Traffic Crash Evolution Characteristic Analysis and Spatiotemporal Hotspot Identification of Urban Road Intersections. *Sustainability* **2018**, *11*, 160. [CrossRef]
61. Muduli, K.; Ghosh, I. Predicting pedestrian-vehicle interaction severity at unsignalized intersections. *Traffic Inj. Prev.* **2025**, *26*, 252–261. [CrossRef] [PubMed]
62. Ni, J.; Chen, J.; Xie, W.; Shao, Y. The impacts of the traffic situation, road conditions, and driving environment on driver stress: A systematic review. *Transp. Res. Part F Traffic Psychol. Behav.* **2024**, *103*, 141–162. [CrossRef]
63. Borucka, A.; Kozłowski, E.; Oleszczuk, P.; Świderski, A. Predictive analysis of the impact of the time of day on road accidents in Poland. *Open Eng.* **2021**, *11*, 142–150. [CrossRef]
64. Benedek, J.; Ciobanu, S.M.; Man, T.C. Hotspots and social background of urban traffic crashes: A case study in Cluj-Napoca (Romania). *Accid. Anal. Prev.* **2016**, *87*, 117–126. [CrossRef] [PubMed]
65. Steenberghen, T.; Aerts, K.; Thomas, I. Spatial clustering of events on a network. *J. Transp. Geogr.* **2010**, *18*, 411–418. [CrossRef]

66. Ismael, K.S.; Razzaq, N.A. Traffic accidents analysis on dry and wet road bends surfaces in greater Manchester-UK. *Kurd. J. Appl. Res.* **2017**, *2*, 284–291. [CrossRef]
67. Cappelli, G.; Nardoianni, S.; D'Apuzzo, M.; Nicolosi, V. Analysis of Contributing Factors influencing Pedestrian Crash Severity: A case study in Rome, Italy. *Transp. Res. Procedia* **2025**, *91*, 798–805. [CrossRef]

Disclaimer/Publisher's Note: The statements, opinions and data contained in all publications are solely those of the individual author(s) and contributor(s) and not of MDPI and/or the editor(s). MDPI and/or the editor(s) disclaim responsibility for any injury to people or property resulting from any ideas, methods, instructions or products referred to in the content.